

IAEA-TECDOC-1499

***Intercomparison of techniques for  
inspection and diagnostics of  
heavy water reactor pressure tubes  
Flaw detection and characterization***



**IAEA**

International Atomic Energy Agency

May 2006

IAEA-TECDOC-1499

***Intercomparison of techniques for  
inspection and diagnostics of  
heavy water reactor pressure tubes  
Flaw detection and characterization***



**IAEA**

International Atomic Energy Agency

May 2006

The originating Section of this publication in the IAEA was:

Nuclear Power Technology Development Section  
International Atomic Energy Agency  
Wagramer Strasse 5  
P.O. Box 100  
A-1400 Vienna, Austria

INTERCOMPARISON OF TECHNIQUES FOR INSPECTION AND DIAGNOSTICS OF  
HEAVY WATER REACTOR PRESSURE TUBES:  
FLAW DETECTION AND CHARACTERIZATION

IAEA, VIENNA, 2006  
IAEA-TECDOC-1499  
ISBN 92-0-105606-0  
ISSN 1011-4289

© IAEA, 2006

Printed by the IAEA in Austria  
May 2006

## FOREWORD

Nuclear power plants with heavy water reactors (HWRs) comprise nine percent of today's operating nuclear units, and more are under construction. Efficient and accurate inspection and diagnostic techniques for various reactor components and systems are an important factor in assuring reliable and safe plant operation.

To foster international collaboration in the efficient and safe use of nuclear power, the IAEA conducted a Coordinated Research Programme (CRP) on Inter-comparison of Techniques for HWR Pressure Tube Inspection and Diagnostics. This CRP was carried out within the frame of the IAEA Department of Nuclear Energy's Technical Working Group on Advanced Technologies for HWRs (the TWG-HWR). The TWG-HWR is a group of experts nominated by their governments and designated by the IAEA to provide advice and to support implementation of the IAEA's project on advanced technologies for HWRs.

The objective of the CRP was to inter-compare non-destructive inspection and diagnostic techniques, in use and being developed, for structural integrity assessment of HWR pressure tubes. During the first phase of this CRP, participants have investigated the capability of different techniques to detect and characterize flaws. During the second phase of this CRP, participants collaborated to detect and characterize hydride blisters and to determine the hydrogen concentration in Zirconium alloys. The intent was to identify the most effective pressure tube inspection and diagnostic methods, and to identify further development needs.

The organizations that have participated in this CRP are:

- The Comisión Nacional de Energía Atómica (CNEA), Argentina;
- Atomic Energy of Canada Ltd. (AECL); Chalk River Laboratories (CRL), Canada;
- The Research Institute of Nuclear Power Operations (RINPO), China National Nuclear Corporation (CNNC), China;
- Bhabha Atomic Research Centre (BARC), India;
- The Korea Electric Power Research Institute (KEPRI), Republic of Korea;
- The Korea Atomic Energy Research Institute (KAERI), Republic of Korea;
- The National Institute for Research and Development for Technical Physics (NIRDTP), Romania; and
- Nuclear Non-Destructive Testing Research and Services (NNDT), Romania.

This TECDOC reports the results of the collaboration on flaw detection and characterization (Phase 1). A companion publication reports results of the collaboration on characterizing hydride blisters and determining the hydrogen concentration in Zirconium alloys (Phase 2).

The IAEA officer responsible for this publication was J. Cleveland of the Division of Nuclear Power.

### *EDITORIAL NOTE*

*The use of particular designations of countries or territories does not imply any judgement by the publisher, the IAEA, as to the legal status of such countries or territories, of their authorities and institutions or of the delimitation of their boundaries.*

*The mention of names of specific companies or products (whether or not indicated as registered) does not imply any intention to infringe proprietary rights, nor should it be construed as an endorsement or recommendation on the part of the IAEA.*

## CONTENTS

|        |  |    |
|--------|--|----|
| 1.     | INTRODUCTION.....  | 1  |
| 1.1.   | Background, and conduct of this CRP .....                                      | 1  |
| 1.2.   | Importance of inter-comparison of PT inspection and diagnostic techniques..... | 2  |
| 1.3.   | Participations from the various laboratories.....                              | 3  |
| 1.3.1. | Argentinean participation .....  | 3  |
| 1.3.2. | Indian participation.....  | 3  |
| 1.3.3. | Korean participation .....   | 3  |
| 1.3.4. | Romania-NIRDTP participation.....  | 4  |
| 1.3.5. | Romania-NNDT participation.....  | 4  |
| 1.3.6. | Chinese participation .....  | 5  |
| 1.3.7. | Canadian participation.....  | 5  |
| 1.4.   | Summary of sample preparation and description.....                             | 5  |
| 1.4.1. | Argentinean sample (ARG1).....   | 5  |
| 1.4.2. | Indian sample (IND1).....  | 6  |
| 1.4.3. | Korean sample (KOR1).....  | 6  |
| 1.4.4. | Romanian sample (ROM2).....  | 6  |
| 1.4.5. | Chinese sample (CHI1) .....  | 6  |
| 1.4.6. | Canadian samples (CAN1 and CAN2).....  | 7  |
| 1.5.   | Inspection and diagnostic techniques .....                                     | 7  |
| 1.5.1. | Argentina .....  | 7  |
| 1.5.2. | India.....   | 7  |
| 1.5.3. | Republic of Korea.....   | 7  |
| 1.5.4. | Romania-NIRDTP .....   | 8  |
| 1.5.5. | Romania-NNDT .....   | 8  |
| 1.5.6. | Canada .....   | 8  |
| 2.     | FLAW DETECTION AND CHARACTERIZATION .....                                      | 10 |
| 2.1.   | Flaw description in PT samples .....   | 10 |
| 2.1.1. | Argentinean sample (ARG1).....   | 10 |
| 2.1.2. | Indian sample (IND1).....  | 13 |
| 2.1.3. | Korean sample (KOR1).....  | 15 |
| 2.1.4. | Romanian sample (ROM2).....  | 17 |
| 2.1.5. | Chinese sample (CHI1) .....  | 20 |
| 2.1.6. | Canadian samples (CAN1 and CAN2).....  | 23 |
| 2.2.   | Inspection and diagnostics techniques .....                                    | 26 |
| 2.2.1. | Argentina .....  | 26 |
| 2.2.2. | India.....   | 26 |
| 2.2.3. | Republic of Korea.....   | 28 |
| 2.2.4. | Romania-NIRDTP .....   | 28 |
| 2.2.5. | Romania-NNDT .....   | 30 |
| 2.2.6. | Canada .....   | 33 |
| 2.3.   | Assessment of results .....  | 35 |
| 2.3.1. | Flaw location .....  | 36 |
| 2.3.2. | Flaw orientation.....  | 36 |
| 2.3.3. | Flaw detection and sizing.....   | 36 |
| 2.3.4. | Flaw characterization.....   | 41 |

|                                     |                                      |    |
|-------------------------------------|--------------------------------------|----|
| 3.                                  | DISCUSSION OF RESULTS .....          | 42 |
| 4.                                  | CONCLUSIONS AND RECOMMENDATIONS..... | 44 |
| 4.1.                                | Conclusions .....                    | 44 |
| 4.2.                                | Recommendations .....                | 44 |
| APPENDIX I.                         | GLOSSARY .....                       | 47 |
| REFERENCES                          | .....                                | 55 |
| CONTRIBUTORS TO DRAFTING AND REVIEW | .....                                | 57 |

ATTACHED CD-ROM:SAMPLE SUMMARY REPORTS OF PRESSURE TUBE SAMPLES

## 1. INTRODUCTION

### 1.1. Background, and conduct of this CRP

The pressure tubes (PTs) of heavy water reactors (HWRs) operate in a high-temperature high-pressure aqueous environment and are subjected to fast neutron irradiation. These conditions lead to degradations in the PTs with respect to i) dimensional changes (creep and growth), ii) deterioration of mechanical properties (hardening and embrittlement) thereby reducing their flaw tolerance, iii) the growth of existing flaws, which were too small or ‘insignificant’ at the time of installation, and iv) initiation and growth of new flaws. The PTs, which are made of Zirconium alloy (Zircaloy-2 or Zr-2.5% Nb), also undergo corrosion in aqueous environment during service. This releases hydrogen, a part of which gets absorbed in the PT material. The absorbed hydrogen is responsible for the two most commonly observed degradation mechanisms that can limit the life of a PT: delayed hydride cracking (DHC) and hydride blister formation and cracking. In HWRs with Zircaloy-2 PTs, an additional mechanism in the form of accelerated oxidation and hydriding can lead to its premature retirement from service, when the oxide layer thickness on its inner surface exceeds the threshold limit.

The PT integrity is central to the safety of HWRs. In order to ensure the PT integrity at all times during their service, they are periodically examined by non-destructive examination (NDE) techniques. These inspections provide valuable information on the presence or absence of flaws in the PTs and their characteristics to designers, plant operators and regulatory authorities for fitness-for-service assessment. NDE methodologies for in-service inspection of PTs have been developed and implemented on in-service inspection tools in several countries operating HWRs.

The International Atomic Energy Agency (IAEA) convened two meetings to provide a forum for technical discussion and exchange of information and experience on HWR PT maintenance and replacement, and to provide recommendations to the IAEA for future cooperative activities in this area. These recommendations were considered at the first meeting of the International Working Group on Advanced Technologies for Heavy Water Reactors (IWG-HWR — now called the Technical Working Group on Advanced Technologies for HWRs), held in Vienna, in June 1997. At this meeting, the IWG-HWR advised the IAEA to convene a consultancy to formulate a coordinated research programme (CRP) to address the application of advanced technologies to the safety and reliability of HWRs. The consultancy held at the IAEA in July 1999 formulated the CRP entitled Inter-comparison of Techniques for Pressure Tube Inspection and Diagnostics. The CRP was divided in two Phases: Phase 1 dealing with ‘Flaw characterization by in situ NDE techniques’ and Phase 2 with ‘Blister characterization by in situ NDE techniques’ and ‘Determination of hydrogen in Zirconium alloy components’.

Phase 1 of the CRP was conducted in a round-robin manner. The participating laboratories prepared PT samples containing artificial flaws resembling real defects of concern. The flaws on the outside surface were hidden by a cover to facilitate blind testing. All samples had to be inspected from the inside surface, as in real conditions. The samples, after examination by participating laboratories, were returned to the originating laboratory, which determined ‘flaw truth’ in its sample. The originating laboratory analysed the sample inspection reports from investigating laboratories and compared the NDE flaw sizing estimates with their true values. The objective of this analysis was to identify the ‘best’ NDE methods for detection, location and sizing of various types of flaws in PTs. For Phase 2, PT samples containing hydride blisters and another set containing known amount of hydrogen were circulated to the participating laboratories. The results of investigations were analysed to identify reliable and

effective techniques for blister characterization and determination of hydrogen concentration in PTs.

This TECDOC presents to the HWR community the capability of NDE techniques, existing and under development, for flaw detection and characterization that were examined during Phase 1 of this CRP. A companion TECDOC presents the results for hydride blister characterization and determination of hydrogen concentration in PTs achieved during Phase 2 of this CRP.

Most of the techniques examined in Phase 1 are well established and are regularly used during in-service inspection of PTs. The inter-comparison of these techniques provides a platform for identifying a particular NDE technique (or a set of techniques), which is more accurate and reliable as compared to others for a specified task. The CRP also witnessed some new NDE methodologies, which can be implemented on in-service inspection tools. These new techniques could complement the existing ones to overcome their limitations, thereby improving the reliability and accuracy of in-service inspection. Finally, this TECDOC identifies future areas of research and development and opens up new avenues for technical collaboration within the HWR community to overcome the challenges faced in PT inspection and diagnostics.

## **1.2. Importance of inter-comparison of PT inspection and diagnostic techniques**

Periodic in-service inspection of PTs by NDE techniques is one of the regulatory requirements for HWRs. The objectives of these inspections are to detect, locate and characterize the flaws in PTs and provide information for fitness-for-service assessment. To assure the structural integrity of PTs at all times during service, it is essential to employ NDE techniques that can reliably detect all the 'significant' flaws and characterize them accurately. In order to assess the effectiveness of these techniques for their intended purpose, it is important that they are periodically subjected to 'blind tests' on PT samples containing known flaws. This CRP on 'Inter-comparison of Techniques for Pressure Tube Inspection and Diagnostics' gave the opportunity for the participating laboratories to prepare their own PT samples containing flaws and carry out blind tests on PT samples prepared by others.

Because these were blind tests, the inspection teams, which examined PT samples, were unaware about the number, location and characteristics of flaws in the samples. This situation is similar to the one faced during in-service inspection of PTs in operating HWRs. The results of examination on PT samples can thus be directly correlated with the effectiveness of NDE techniques for detection and characterization of flaws. A good detectability and accurate characterization would strengthen the confidence in the technique(s) employed, while poor detectability and inaccurate characterization would give a feedback to the laboratory that the existing technique(s) need(s) improvement(s) or new ones should be developed.

The inter-comparison of NDE techniques based on the results of investigation of PT samples highlights the most reliable and accurate NDE method (ultrasonic, eddy-current or a combination of both) and also a specific technique for that NDE method (time-of-flight monitoring, amplitude monitoring, C-scan image, etc.) for detection and characterization of various kinds of flaws encountered in PTs. This information is useful for the HWR community to improve the tools being used for PT inspection and diagnostics, by modifying the existing techniques or adapting new ones, so that the inspection is carried out in the most effective manner. The inter-comparison of NDE techniques also helps in identifying those areas where none of the existing techniques are reliable or effective to the desired level. It identifies areas of research for future collaboration in this field.

### **1.3. Participations from the various laboratories**

The ultrasonic testing (UT) and eddy-current testing (ET) terms are defined in the glossary in Appendix I.

#### ***1.3.1. Argentinean participation***

The CNEA produced flaws on a piece of PT (ARG1) provided by India. The inspection team performed UT examinations of the samples from all participating countries.

The CNEA hosted the second Research Coordination meeting (RCM) in Buenos Aires, Argentina, in May 2001. Participants from Argentina, Canada, China, India, Rep. of Korea, Romania, and the IAEA attended this meeting. The purpose of the meeting was to review progress of Phase 1 with respect to sample preparation, transfer and inspection, and prepare an action plan for Phase 2.

During this CRP, laser-optical techniques were also tested, investigating their capability as a NDE technique for PT inspection.

#### ***1.3.2. Indian participation***

Artificial flaws that duplicate real defects of concern were machined in an approximately 500 mm long PT sample. Blank PT pieces of similar length were provided to Argentina and Peoples Rep. of China, at no cost, so that they could embed flaws in them and then put these samples into circulation.

India examined PT samples from Argentina, Canada, China, Rep. of Korea, Romania and its own sample. The examination was carried out in immersion conditions using a specially-designed scanning system. An inspection head containing UT and ET probes was also designed and fabricated. The flaws in PT samples were fully characterized with respect to their location, orientation, size and type. Conventional and advanced UT techniques were employed for this purpose. A detailed sample inspection report was prepared for each sample and sent to the originating laboratories.

For the Indian PT sample (IND1), the ‘flaw truth’ (true flaw dimensions) was determined for all the machined flaws. The IND1 sample inspection reports from all the participating laboratories were analysed and a detailed sample summary report was prepared. India provided an extensive analysis of the inspection results, which was adopted in this TECDOC, to help identify the most effective and reliable NDE methods for detection, location and sizing of various types of flaws in PTs. India prepared the draft of the sections of this TECDOC on ‘Background and conduct of this CRP’ and ‘Importance of inter-comparison of PT inspection and diagnostics techniques’. India also prepared the sample summary report for the Chinese sample (CHI1).

#### ***1.3.3. Korean participation***

The Rep. of Korea prepared the KOR1 sample and circulated it to the six participants. The six KOR1 sample inspection reports were analysed and a detailed sample summary report was prepared. This report provides an analysis of the flaw delectability and sizing accuracy of applied NDE methods.

The Rep. of Korea also examined PT samples from Argentina, Canada, China, Romania, and its own sample. The examinations were carried out using a custom-made scanning system equipped with an ET send-receiver probe. The artificial flaws in PTs were characterized with respect to their locations, size and shape. Detailed sample inspection reports were prepared for each sample and sent to the originating laboratories.

#### ***1.3.4. Romania-NIRDTP participation***

In 2000, the IAEA approved the participation of the National Institute of Research and Development for Technical Physics (NIRDTP) in this CRP. The NIRDTP conducted their activities based on annual research contracts between IAEA and the NIRDTP. The NIRDTP accomplished all the contracted tasks as described below:

- (a) Designed, built and employed an ET send-receive transducer with rotating magnetic field (RMF) for the inspection of the PT samples [1], [2], [3], [4].
- (b) Completed model and solved the forward problem [5], [6], [7].
- (c) Solved inverse problem using numerical code for evaluation of discontinuities in PT samples [8], [9].
- (d) Examined all samples circulated during the CRP, except ROM2, and prepared the corresponding sample inspection reports. The shorter length of this sample as well as the presence of a material transition prevented an inspection with the available ET system.

#### ***1.3.5. Romania-NNDT participation***

Romania-NNDT designed and constructed specialized equipment, the ISIS-UT&ET Laboratory Multichannel Inspection System for examination of PT samples. It is a complex laboratory system to simulate fuel channel inspections. The functional structure of this system integrates all applicable flaw detection and sizing UT and ET methods addressed by the Periodic Inspection Standard CAN/CSA N285.4 [10], referred in the rest of the document as the Canadian Standard. For this system, Romania-NNDT developed dedicated software for data acquisition and analysis.

The ISIS-UT&ET equipment was completed and improved by implementation of the new inspection methodology and techniques elaborated in the framework of this CRP.

Romania-NNDT examined all samples circulated during the CRP (ARG1, CAN1/2, CHI1, IND1, KOR1 and ROM2). The objective of these inspections was to detect size and characterize the intentional and non-intentional flaws existing in the samples, applying the examination methodology, calibration requirements, and recording criteria specified in the Canadian Standard. The reporting of the detected indications was made according to the requirements of the Canadian Standard, and also respected the “Terms of Reference” established in the framework of the CRP.

For the PT sample inspections, conventional (routinely used) inspection methods as well as new advanced methods were applied in order to test their capability, accuracy and reliability. All sample inspection reports completed by Romania-NNDT during this CRP contain very detailed description of the inspection results, and extensive appendices with the collected data for all reportable indications (including the non-intentional indications).

Romania-NNDT designed and constructed its own sample (ROM2) introducing flaws that permit the characterization of the intrinsic performances of the inspection methodology applied by the investigating laboratories.

Romania-NNDT attended and participated actively in all the RCMs.

### ***1.3.6. Chinese participation***

China participated in the CRP up to April 2004, at which time China then announced their withdrawal due to a budget cut within their organization. Before that, China had prepared a sample (CHI1) from a piece of PT provided by India. After their withdrawal, China granted continuation of the circulation of the sample as originally planned. Canada provided the 'flaw truth' for this sample and India wrote the sample summary report. Before its withdrawal, China had examined samples from two countries (Canada and Rep. of Korea) and was able to provide the corresponding sample inspection reports to the originating laboratories for inclusion in the sample summary reports. It was agreed not to assess China's NDE capability in this TECDOC due to limited inspection results.

### ***1.3.7. Canadian participation***

Canada led Phase 1 of the CRP. Canada prepared jointly with Argentina and presented to the TWG-HWR in Vienna (June 2004) a case for an extension of the CRP (until end of 2005); this request was approved. Canada assisted in the organization of all meetings and hosted the final RCM.

Canada defined what the reference flaws should be and gave information for representative flaws and how to manufacture them. Canada provided two samples to cover a wide range of flaws, helped coordinate the rotation of all samples and resolve other issues as they occurred all along the CRP.

Canada performed on all samples UT examinations of all flaws, ET and profilometry examinations of the ID flaws.

Beyond conducting profilometry examinations on their own samples (CAN1 and CAN2) to provide full characterization of all flaws, Canada did the same for the KOR1 and CHI1 samples for the respective sample summary reports to be completed on time.

Canada provided a template and scope for the sample inspection reports as well as recommendations for the sample summary reports. Canada produced the draft assessment/analysis part of this TECDOC.

## **1.4. Summary of sample preparation and description**

All PT samples were made as per the requirements decided upon at the opening meeting of the CRP. All samples were made of un-irradiated Zr-2.5% Nb PT material.

### ***1.4.1. Argentinean sample (ARG1)***

The ARG1 sample was made from a piece of PT provided by India. A total of 20 flaws were machined in the sample. Out of these, 16 flaws were on the OD surface and the remaining four on the ID surface of the PT. The flaws were classified by type (axial flaws, circumferential flaws, etc).

#### **1.4.2. Indian sample (IND1)**

Artificial notches and grooves were machined in the IND1 sample in such a manner that they closely resemble the real defects. The PT sample also contained reference notches for calibration as required by the Canadian Standard. The IND1 sample has a total of 17 flaws, 12 on the OD surface and five on the ID surface. These flaws can be categorized in seven categories: i) DHC in axial direction on ID and OD surfaces, ii) DHC in circumferential direction on ID and OD surfaces, iii) DHC, oblique to the tube axis, iv) lap-type or laminar defect near ID, OD and mid-wall v) smooth debris fret, vi) sharp debris fret and vii) bearing-pad fret.

#### **1.4.3. Korean sample (KOR1)**

Defects, such as fretting damage and crack-like notches representative of those that can arise in CANDU reactors were introduced into the KOR1 sample. It contained a total of 12 intentional flaws, eight on the OD surface and four on the ID surface. All flaws on the inner and external surfaces were electro-discharge machining (EDM) notches with rectangular and semi-elliptical profiles. A range of flaw sizes and orientations was selected. A few unintentional scratches (handling at Wolsong NPP) were present on internal and external surfaces of the sample.

#### **1.4.4. Romanian sample (ROM2)**

The main design objective of the ROM2 sample was to provide a sample containing “families” of flaws of various dimensions for comparison of the intrinsic performances of the examination methods used by the investigating laboratories, in terms of detection sensitivity, resolution and sizing accuracy. The ROM2 sample consisted of three PT rings containing 60 artificial flaws machined through different mechanical processes: drilling, milling, EDM. The families of machined flaws were radial round and flat bottom holes, axial holes, axial and circumferential holes with round, flat or angled (V-form) channels. The ROM2 sample also contained a number of flaws close to the edge of the PT to evaluate the edge effects, simulating flaws located in the rolled joint region. Some flaws were more representative of real flaws, like the flat, and angled (V-form) ID channels, which simulate debris flaws.

Because of the small dimensions and high number of machined flaws, the ROM2 sample was especially intended to test the performance of UT techniques, but its usefulness for characterising some aspects of the ET techniques was also significant.

The ROM2 sample does not contain reference flaws for calibration according to the Canadian Standard. It was assumed that calibration could be achieved using a separate piece of PT.

#### **1.4.5. Chinese sample (CHI1)**

The CHI1 sample contained the four calibration slots (axial and circumferential ID and OD) as per the Canadian Standard. A total of 26 flaws were machined in this sample. Out of these, 21 flaws were on the OD surface, and the remaining five on the ID surface. No flaws were added within wall. The flaws were classified by type (axial flaws, circumferential flaws, flaws with tilt, oblique flaws, lap-type or laminar flaws).

#### **1.4.6. Canadian samples (CAN1 and CAN2)**

Both samples (CAN1 and CAN2) contained the four calibration notches as well as the three normal beam calibration slots as per the Canadian Standard. Both samples had multiple flaws of various types on ID and OD surfaces, 17 in CAN1 sample and five in CAN2 sample, as representative as possible to flaws encountered in-service: OD axial and circumferential semi-elliptical (simulating DHC), ID axial debris frets of varying complexity with and without DHC, ID axial and circumferential undercut with and without DHC, ID bearing pad frets of various complexity with and without DHC in a corner and an OD axial scratch (simulating an installation scratch). Replicas of each flaw were taken at the end of the round-robin exercise to obtain a precise characterization of each flaw.

### **1.5. Inspection and diagnostic techniques**

#### **1.5.1. Argentina**

Argentina used UT examinations for detection, location and characterization of flaws in the various PT samples. The shear wave pulse echo technique was employed using four transducers, two (in opposite directions) in the axial direction more sensitive to circumferential indications and two (in opposite directions) in the circumferential direction more sensitive to axial indications. The four reference notches from the Canadian Standard (ID axial, ID circumferential, OD axial and OD circumferential) were used for calibration and setting of the detection level.

#### **1.5.2. India**

UT examination was carried out using four angle beam shear wave transducers (10 MHz) and two normal beam transducers, one focused on the OD surface (10 MHz) and the other on the ID surface (20 MHz). The techniques employed for flaw detection included angle beam pulse-echo, amplitude drop monitoring during angle beam pitch-catch and normal beam backwall drop. The scanning sensitivity for pulse-echo UT examination was set two to four times above the reference sensitivity. The recording criteria was set at 6dB above the noise level, which is very stringent as compared to conventional criteria of 20% or 50% of reference level. For the amplitude drop techniques (normal and angle beam pitch-catch), any indication showing a drop of more than 5 to 10% of the reference signal was evaluated. Once the flaw was detected, length, width and depth were sized. The flaw length and width were determined by the 6dB drop technique using angle beam and normal beam signals. The flaw depths were determined by time-of-flight using angle beam pitch-catch and normal beam examinations. Records for the flaws included B-scan images and time-of-flight and amplitude plots.

#### **1.5.3. Republic of Korea**

Korea used an ET method for flaw detection and characterization. The send-receiver ET transducer was primarily designed to detect ID flaws in the PT samples. This ET transducer consists of two coils. One coil acts as a sender, and the other coil as a receiver. The primary frequency of 60 kHz was used for detection of the ID flaws. A second frequency of 20 kHz was selected to attempt the detection of the OD flaws. 100 kHz was used as an additional frequency.

The calibration set-up for flaw sizing used 20%, 50%, and 70% through-wall notches. The flaw depths were estimated by measuring the phase angle of the flaw signals. The flaw widths and lengths were estimated using the 6dB drop technique. The recording criterion was set at

50% above the reference sensitivity. Any signals over reference level was recorded and evaluated.

#### **1.5.4. Romania-NIRDTP**

Romania-NIRDTP examined PT samples by ET using a RMF send-receive probe. The experimental and theoretical aspects of this technique need to be further refined.

The emission part of this transducer is made of three rectangular coils, wound with 120° angle between them, star connected and driven by a three-phased alternative current. The magnetic field created by the three coils is a rotating field of a frequency equal to that of the three-phase current. The receiver is made of an array of 24 identical coils equally spaced circumferentially.

Three programmable function generator cards supply the circuit with the three-phase alternative current, as well as the reference for synchronous detection. The signals are amplified and applied to the transmitter creating a RMF. The 24 receiver coils are consecutively interrogated and acquired by a PC.

The RMF transducer and the control equipment were integrally designed and constructed at NIRDTP. The equipment allows to clearly detect a 0.1 mm wide and 0.1 mm deep slot placed on the ID or on the OD of a PT with signal to noise ratio better than 3:1.

#### **1.5.5. Romania-NNDT**

The PT samples of this CRP were examined using various UT techniques. The inspection head contains 10 MHz transducers for angle beam (45° shear waves, double skip/W pattern — four angle beam transducers, one pair looking axially and the other looking circumferentially) and normal beam transducers (25 MHz focused on ID, 25 MHz focused on OD, 25 MHz focused on mid-wall, 10 MHz focused on OD, and 10 MHz focused on mid-wall).

Angle beam examination was carried out in both pulse-echo (reflection) mode as well as pitch-catch (transmission) mode. In the case of pulse-echo examination, the echo signal is generated by the reflected ultrasound from a flaw; the pulse-echo examination was used especially for flaw evaluation, but it also gave good results for detection. The pitch-catch mode was used for detection and for location of flaws (ID, OD, within wall). In pitch-catch mode, the amplitude drop of the ultrasound beam received at the receiving transducer is recorded. It gave very good results, even for flaws with unfavourable orientations.

For the normal beam examinations, flaw detection was based on the amplitude drop and time-of-flight of the first OD backwall echo, or on the amplitude and time-of-flight of the echo reflected by the flaw. Also, in the case of ID surface profiling, the amplitude and time-of-flight of the surface echo are monitored.

#### **1.5.6. Canada**

Flaw detection and characterization with UT was performed with four shear wave transducers and one normal beam probe assembled in a cluster. A 20 MHz normal beam transducer was also used for surface profiling of the ID flaws.

Flaw detection and characterization with ET was performed with two surface probes: the first, a Ghent 1 (G1) [11], is designed to compensate for lift-off noise, thereby improving signal-to-

noise for detection of flaws; and the second, a transmit-dual receive (TDR) probe is used to differentiate between axially and circumferentially oriented flaws. Both the G1 and TDR probes satisfy the primary detection and sizing requirements for a PT inspection. ET was used to detect and size ID flaws only.

Both ET and UT use sophisticated data acquisition and analysis software. ET results combined with information obtained from UT provide increased confidence in interpretation of PT inspection data [12].

Profilometry was performed on all ID flaws, as is the case for an in-service inspection. Profilometry was also used as the examination technique to provide full characterization of all flaws (OD and ID) for three samples.

All these techniques are well established and have been used in-service for many years.

## 2. FLAW DETECTION AND CHARACTERIZATION

### 2.1. Flaw description in PT samples

All samples were made from un-irradiated Zr-2.5% Nb pieces of PT. Most samples were 103.4 mm ID and 112 mm OD (standard size of a PT), and approximately 500 mm long (except ROM2). A punch mark was made very close to one end of each sample. The punch mark indicates the 12 o'clock position and also identifies the face of the tube for making all the measurements. All samples contain flaws on ID and OD surfaces. One sample (ROM2) also contained flaws within wall. Once the flaws were machined, a cover was installed and sealed on the outside to hide the OD flaws. A length of approximately 50 mm of PT was left uncovered at both ends of both samples to facilitate holding the sample in the fixtures during the inspection. No flaws were machined in this zone of 50 mm on either end of the samples, except for ROM2 in which few flaws were machined, from the PT end, in the wall of the PT. The samples were supposed to contain the four calibration notches (axial and circumferential ID and OD notches) as well as the three normal beam calibration slots as per the Canadian Standard. The artificial flaws were machined to be as representative as possible to real flaws encountered in reactor.

Dimensions of all calibration features and flaws were obtained either after manufacturing or at the end of the round-robin exercise to provide the flaw truth for comparison with the various NDE techniques used by the participating countries. Flaw truth was determined by profilometry or measuring microscope.

#### 2.1.1. *Argentinean sample (ARG1)*

The details of flaws in ARG1 sample with respect to their location, orientation, size and characteristics are given in Table 1.

Table 1. Flaw details in ARG1 sample

| Flaw # | Location and Orientation | Flaw Size   |            |            | Characteristics              |
|--------|--------------------------|-------------|------------|------------|------------------------------|
|        |                          | Length (mm) | Width (mm) | Depth (mm) |                              |
| 1      | ID, axial                | 6.1         | 0.3        | 0.136      | calibration slot             |
| 2      | OD, axial                | 6.15        | 0.4        | 0.14       | calibration slot             |
| 3      | ID, circumferential      | 6.2         | 0.3        | 0.152      | calibration slot             |
| 4      | OD, circumferential      | 6.6         | 0.4        | 0.16       | calibration slot             |
| 5      | OD, axial                | 1.4         | 0.65       | 0.7        | flat-bottom calibration slot |
| 6      | OD, axial                | 1.45        | 0.7        | 2.25       | flat-bottom calibration slot |
| 7      | OD, axial                | 1.5         | 0.75       | 3.75       | flat-bottom calibration slot |
| 8      | OD, axial                | 34.5        | 0.55       | 0.145      | long and shallow notch       |
| 9      | OD, circumferential      | 29.2        | 0.5        | 2.05       | long and deep curved notch   |
| 10     | OD, round                | 2.5         | 2.5        | 1.522      | dent/flat-bottom             |
| 11     | OD, round                | 2.35        | 2.35       | 0.53       | dent/flat-bottom             |
| 12     | OD, round                | 2.35        | 2.35       | 2.03       | dent/flat-bottom             |
| 13     | OD, round                | 2.2         | 2.2        | 1.035      | dent/flat-bottom             |
| 14     | OD, circumferential      | 23.45       | 0.85       | 1.45       | long and deep curved notch   |
| 15     | OD, axial                | 38.25       | 0.6        | 2.4        | long and deep oblique notch  |
| 16     | OD, circumferential      | 27.6        | 0.45       | 1.56       | long and deep oblique notch  |
| 17     | OD, circumferential      | 36.6        | 0.4        | 2.95       | long and deep notch          |
| 18     | OD, circumferential      | 19.55       | 0.4        | 0.81       | long and deep notch          |
| 19     | ID, circumferential      | 10          | 2.1        | 1.938      | long and deep notch          |
| 20     | ID, axial                | 3.9         | 1          | 0.938      | short and deep notch         |

The method employed to get the flaw truth was direct profilometry for the OD flaws and measurement of the replicas using a microscope for the ID flaws.

Figure 1 shows photographs of some of the OD flaws present in the ARG1 sample.

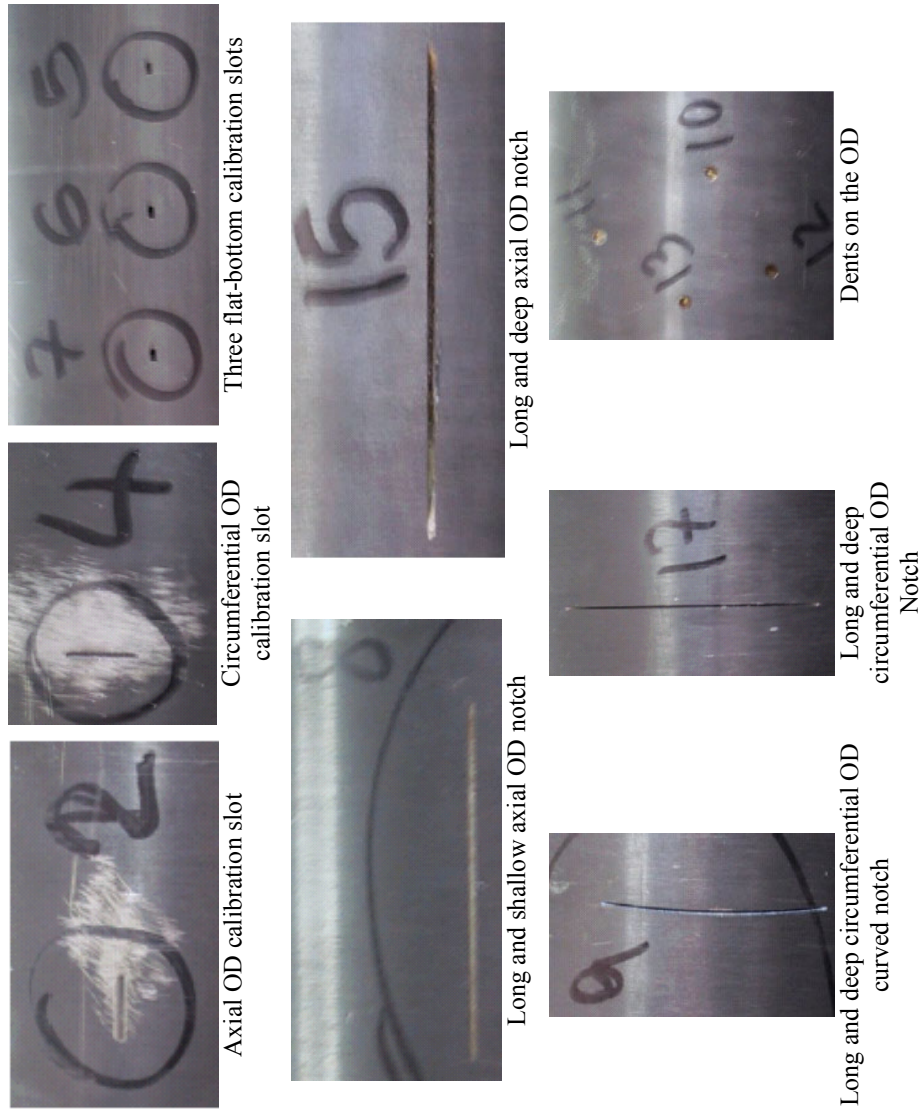


FIG. 1. Photographs of some of the OD features machined in the ARG1 sample.

### 2.1.2. Indian sample (IND1)

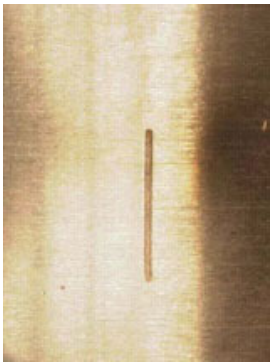
The details of flaws in IND1 sample with respect to their location, orientation, size and characteristics are given in Table 2.

Table 2. Flaw details in IND1 sample

| Flaw # | Location and Orientation | Flaw Size   |            |            | Characteristics                   |
|--------|--------------------------|-------------|------------|------------|-----------------------------------|
|        |                          | Length (mm) | Width (mm) | Depth (mm) |                                   |
| 1      | OD, Oblique at 45°       | 5.84        | 0.21       | 0.16       | DHC                               |
| 2      | ID, equiaxed             | 2.50        | 2.3        | 1.15       | smooth debris fret                |
| 3      | OD, equiaxed             | 1.46        | 0.80       | 0.63       | lap type defect near OD           |
| 4      | ID, axial                | 11.50       | 2.3        | 1.00       | bearing pad fret                  |
| 5      | ID, axial                | 6.00        | 0.4        | 0.22       | reference flaw                    |
| 6      | ID, circumferential      | 6.00        | 0.3        | 0.21       | reference flaw                    |
| 7      | OD, oblique at 20°       | 5.81        | 0.24       | 0.16       | DHC                               |
| 8      | OD, equiaxed             | 1.92        | 1.27       | 3.67       | lap type defect near ID           |
| 9      | ID, axial                | 2.00        | 1.0        | 1.10       | sharp debris fret                 |
| 10     | OD, circumferential      | 5.88        | 0.32       | 0.11       | DHC shallower than reference flaw |
| 11     | OD, axial                | 5.85        | 0.28       | 0.13       | reference flaw                    |
| 12     | OD, circumferential      | 5.76        | 0.27       | 0.14       | reference flaw                    |
| 13     | OD, circumferential      | 11.96       | 0.39       | 0.23       | DHC                               |
| 14     | OD, oblique at 20°       | 5.84        | 0.17       | 0.13       | DHC                               |
| 15     | OD, equiaxed             | 1.62        | 1.15       | 2.14       | lap type defect at mid-wall       |
| 16     | OD, axial                | 5.80        | 0.24       | 0.068      | DHC shallower than reference flaw |
| 17     | OD, axial                | 11.88       | 0.35       | 0.17       | DHC                               |

The dimensions of all the OD flaws were measured using a microscope with an accuracy of 0.01 mm for length and 0.005 mm for width and depth. The dimensions of all the ID flaws were taken from the profilometry results reported by Canada.

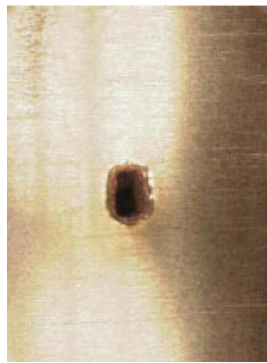
Figure 2 shows photographs of some of the OD and ID flaws present in the IND1 sample.



OD axial reference notch



OD oblique 45°, same size as reference notch



OD equiaxed, 3.67 mm deep



OD circumferential reference notch



OD equiaxed, 0.63 mm deep



ID sharp debris fret



OD oblique 20°, same size as reference notch



OD equiaxed, 2.14 mm deep



ID bearing pad fret

*FIG. 2. Photographs of some of the OD and ID features machined in the INDI sample.*

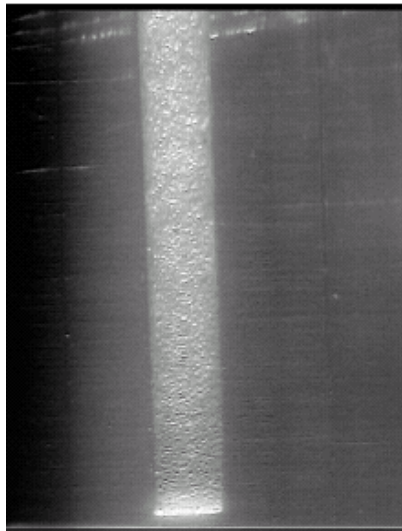
### 2.1.3. Korean sample (KOR1)

The details of flaws in KOR1 sample with respect to their location, orientation, size and characteristics are given in Table 3.

Table 3. Flaw details in KOR1 sample

| Flaw # | Location and Orientation | Flaw Size   |            |            | Characteristics                                  |
|--------|--------------------------|-------------|------------|------------|--|
|        |                          | Length (mm) | Width (mm) | Depth (mm) |  |
| 1      | OD, axial                | 6.0         | 0.3        | 0.47       | short notch deeper than calibration slot         |
| 2      | OD, tilted               | 6.0         | 1          | 0.93       | short and deep notch                             |
| 3      | OD, oblique              | 6.5         | 0.3        | 1.01       | short and deep notch                             |
| 4      | OD, circumferential      | 6.0         | 0.3        | 0.41       | short notch deeper than calibration slot         |
| 5      | OD, tilted               | 6.0         | 1.0        | 0.98       | short and deep notch                             |
| 6      | OD, oblique              | 6.5         | 0.3        | 1.04       | short and deep notch                             |
| 7      | OD, axial                | 20.0        | 5.2        | 0.26       | fretting mark                                    |
| 8      | ID, circumferential      | 6           | 0.3        | 0.29       | short notch deeper than calibration slot         |
| 9      | OD, oblique              | 6.0         | 0.4        | 1.07       | short and deep notch                             |
| 10     | ID, circumferential      | 6.0         | 0.3        | 0.23       | short notch similar in depth to calibration slot |
| 11     | ID, axial                | 25.5        | 2.1        | 0.22       | fretting mark                                    |
| 12     | ID, oblique              | 6.5         | 0.2        | 0.23       | short notch similar in depth to calibration slot |

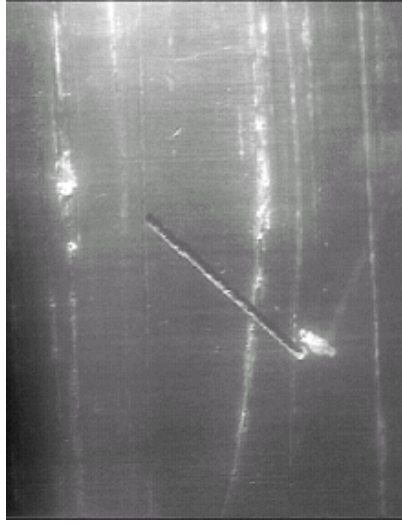
The flaw truth for the KOR1 sample was provided by Canada through profilometry. Figure 3 shows photographs of some of the ID flaws present in the KOR1 sample. Pictures of unintentional scratches and debris frets are included for interest.



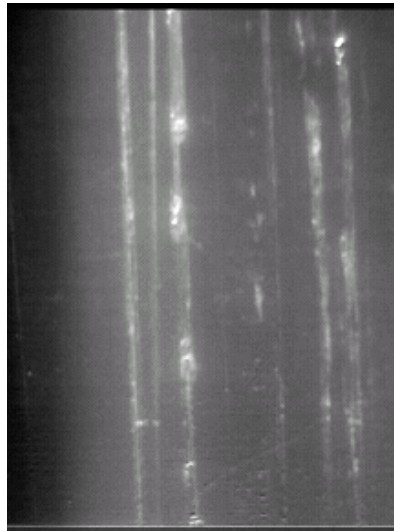
ID axial bearing pad fret



ID circumferential reference notch



ID oblique 45°



Unintentional ID scratches



Unintentional ID debris fret with lift-off



Unintentional ID debris fret with lift-off

*FIG. 3. Photographs of some of the ID features present in the KOR1 sample.*

#### 2.1.4. Romanian sample (ROM2)

The details of flaws in ROM2 sample with respect to their location, orientation, size and characteristics are given in Table 4.

Table 4. Types of flaws contained in ROM2 sample

| PT Ring Code | Ring Height (mm) | Type of Artificial Flaws | Flaw Orientation | 1. Number of Flaws |
|--------------|------------------|--------------------------|------------------|--------------------|
| ROM-2-H      | 12               | round-bottom hole        | axial            | 16                 |
|              |                  | flat-bottom hole         | radial           | 2                  |
|              |                  | through-wall hole        | radial           | 1                  |
|              |                  | EDM channel              | axial            | 2                  |
|              |                  | EDM channel              | circumferential  | 2                  |
| ROM-2-R      | 50               | round-bottom hole        | radial           | 21                 |
|              |                  | milling channel          | circumferential  | 2                  |
|              |                  | milling channel          | axial            | 2                  |
| ROM-2-A      | 14.3             | milling channel          | axial            | 7                  |
|              |                  | milling channel          | axial            | 4                  |
|              |                  | cylindrical long hole    | axial            | 1                  |

Figures 4 and 5 show the ROM2 sample with the three rings.

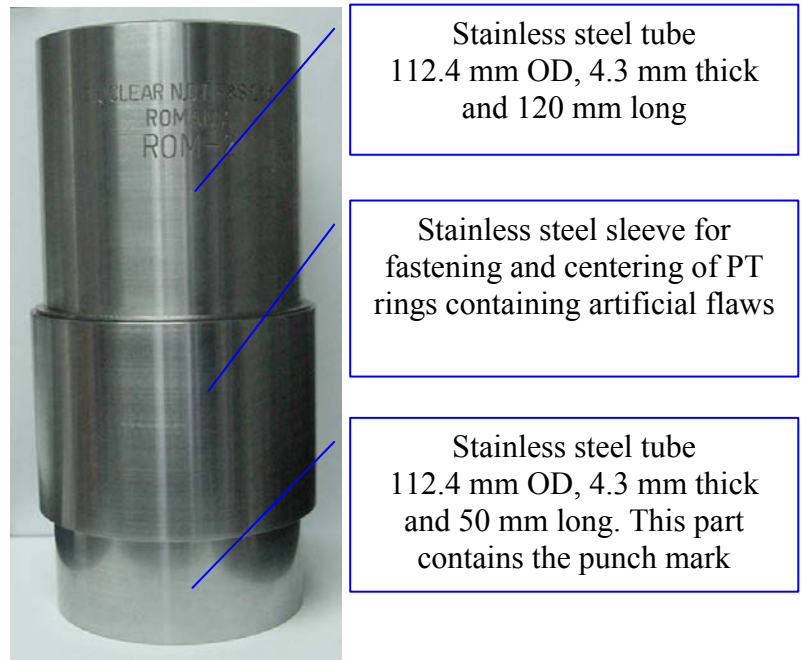


*FIG. 4. Outside view of the ROM2 sample.*

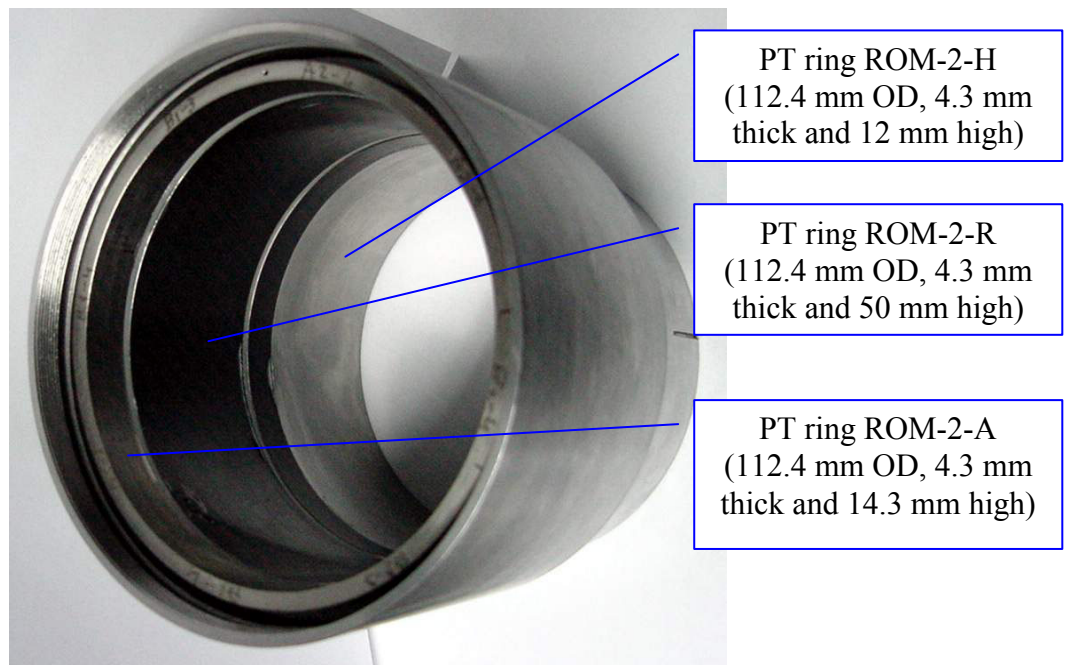


*FIG. 5. Inside view of the ROM2 sample.*

#### 2.1.4.1. *Type and dimensions of flaws in the ROM2 sample*

The ROM2 sample contained the following families of flaws (see enclosed CD for all dimensions and further details about the ROM2 sample):

##### **(I) Radial holes of the following types**

**(I.1) Round-bottom holes** machined on the ROM-2-R ring by drilling with conical-end drill, from the outside of the PT. Optical examination in longitudinal cross-section of holes of this type, machined in the same conditions, demonstrated that their bottom is rounded. Various depths were obtained: 0.4 mm, 0.8 mm and 1.2 mm.

**(I.2) Flat-bottom holes** achieved by EDM from the inside and outside of the PT. There were 2 flaws of this type on the ROM-2-H PT ring, with the same dimensions 1 mm diameter and 0.5 mm in depth.

**(I.3) Through-wall hole** machined by auger drilling. The ROM-2-H PT ring contained one such flaw with a 1 mm diameter.

##### **(II) Axial and circumferential channels of the following types**

**(II.1) Flat-bottom channels** machined by EDM. There were 4 flaws of this type on the ROM-2-H PT ring, two in the axial direction, and two in the circumferential direction, one of each type on ID and OD surfaces. All these flaws are 5 mm long, 0.2 mm wide and 0.1 mm deep.

**(II.2) Round-bottom (U-form) channels** machined by milling. There were 4 flaws of this type on the ROM-2-R PT ring, two in the axial direction on the OD, and two in the circumferential direction (one on the ID and one on the OD). All these channels were about 12 mm long (in the constant depth zone), 0.2 mm wide and 0.1 mm deep. Also, there were seven milling U-form channels, machined with depths between 0.15 mm and 3 mm from the OD on the ROM-2-A PT ring; all these channels are 0.25 mm wide.

**(II.3) Angled (V-form) channels** machined by milling. There were 4 flaws of this type on the ROM-2-A PT ring.

##### **(III) Axial holes**

These were flaws machined in the PT wall by drilling with conical-end auger in the axial direction, from the OD surface. Because of the conical-end auger, the bottom of these holes is rounded. There were 16 flaws of this type on the ROM-2-H PT ring, eight on each ring face.

##### **(IV) Axial long hole**

There was only one hole of 1 mm diameter and 14.3 mm length machined by drilling at mid-wall on the ROM-2-A PT ring.

Figure 6 shows the location of most flaws present in the ROM2 sample. This is an UT C-scan image obtained with the normal beam first backwall amplitude while performing the detection scan.

#### 2.1.4.2. *Dimensional characterization*

As a general remark on flaw dimensions, depending on the machining technology used (auger drilling, milling or EDM), it was observed that the real flaw dimensions were very closed to the dimensions of the tools used (especially for the hole diameters and channel widths). These dimensions are imposed by the applied machining process. The statistical evaluation performed by destructive analysis (optical measurement of the cross-sections) of a statistical set of samples of artificial flaws machined in a similar manner as the round-robin sample flaws, showed that the real flaw dimensions ranged in very tight machining tolerances.

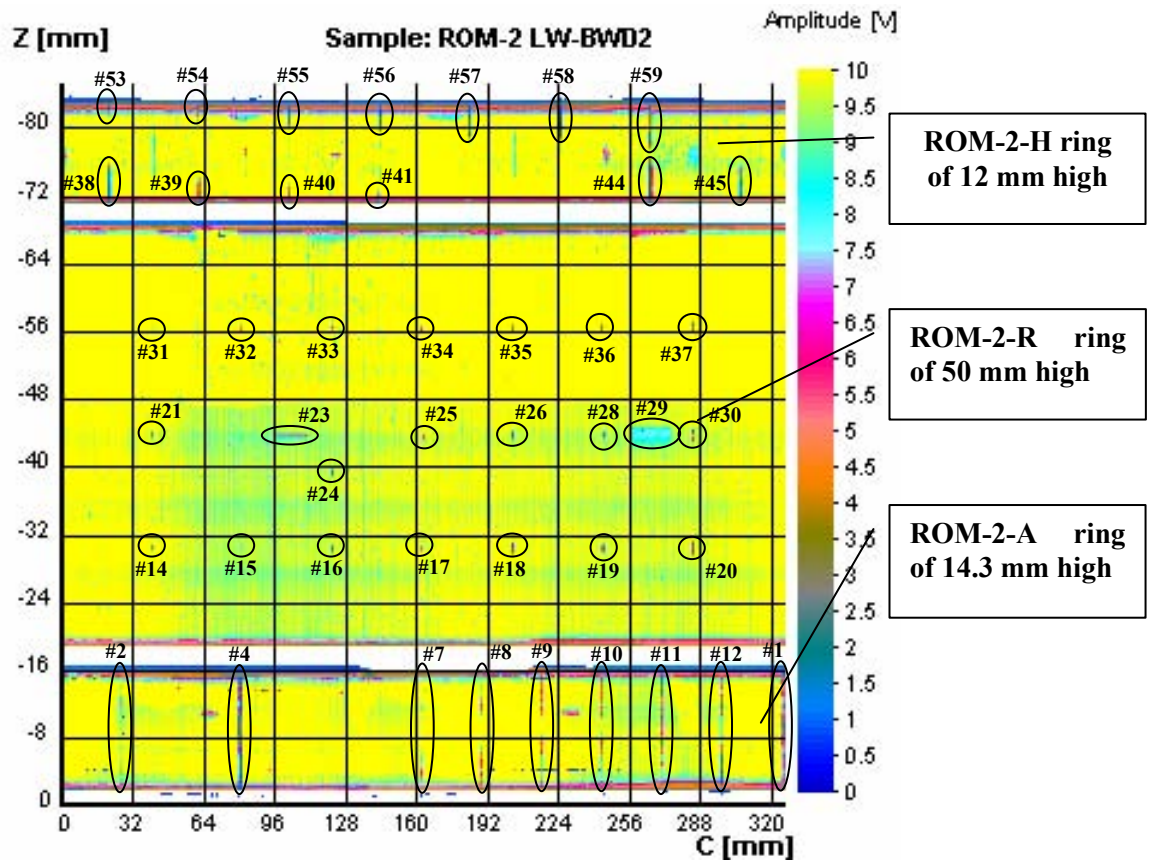


FIG. 6. Flaw location in the ROM2 sample.

The machined flaws were dimensionally characterized by direct optical examination in the case of small depth OD flaws, and by replica measurements in the case of ID flaws and deep OD flaws.

The real depth of the flaws, (shown in the enclosed CD), was verified, also, by accurate time-of-flight UT measurements, using a USIP12 flaw detector and the DTM12 time-of-flight module. The accuracy of these measurements is  $\pm 1$  ns (or, equivalent,  $\pm 0.005$  mm) in the AVERAGE mode, if the temperature is controlled within  $\pm 0.5^\circ\text{C}$ .

### 2.1.5. Chinese sample (CHI1)

The details of flaws in CHI1 sample with respect to their location, orientation, size and characteristics are given in Table 5.

The flaw truth for the CHI1 sample was provided by Canada through profilometry.

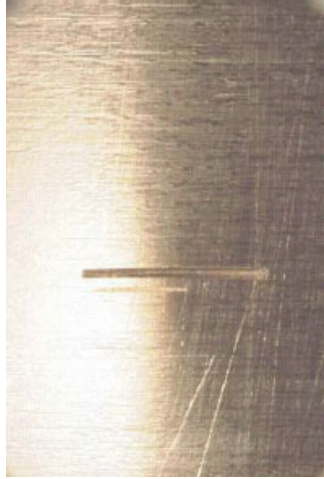
Figure 7 shows photographs of some of the OD flaws present in the CHI1 sample.

Table 5. Flaw details in CHI1 sample

| Flaw # | Location and Orientation    | Flaw Size   |            |            | Characteristics                     |
|--------|-----------------------------|-------------|------------|------------|-------------------------------------|
|        |                             | Length (mm) | Width (mm) | Depth (mm) |                                     |
| 1      | OD, axial                   | 5.0         | 0.5        | 0.58       | short narrow notch                  |
| 2      | OD, axial                   | 6.0         | 0.3        | 0.18       | short narrow notch                  |
| 3      | OD, axial                   | 12.5        | 0.6        | 0.76       | long narrow notch of variable depth |
| 4      | OD, circumferential, tilted | 6.0         | 0.3        | 0.38       | short notch of variable depth       |
| 5      | OD, circumferential         | 6.0         | 0.4        | 0.6        | short notch                         |
| 6      | OD, circumferential         | 5.0         | 0.3        | 0.21       | short shallow notch                 |
| 7      | OD, cross like              | 6.0         | 0.3        | 0.29       | short cross-like notch              |
| 8      | OD, axial                   | 5.5         | 0.3        | 0.22       | short shallow notch                 |
| 9      | ID, axial                   | 6.0         | 0.3        | 0.13       | short shallow notch                 |
| 10     | ID, axial                   | 6.0         | 0.2        | 0.15       | short shallow notch                 |
| 11     | ID, axial                   | 6.0         | 0.3        | 0.19       | short shallow notch                 |
| 12     | OD                          | 10.5        | 5.3        | 0.18       | tilted square large and shallow     |
| 13     | OD, circumferential         | 8.0         | 0.3        | 0.13       | long shallow notch                  |
| 14     | OD, circumferential         | 8.0         | 0.2        | 0.16       | long shallow notch                  |
| 15     | OD, circumferential         | 8.0         | 0.3        | 0.15       | long shallow notch                  |
| 16     | OD, circumferential         | 8.0         | 0.2        | 0.26       | long shallow notch                  |
| 17     | OD, axial                   | 5.5         | 0.2        | 0.15       | short shallow notch                 |
| 18     | OD, axial                   | 5.0         | 0.5        | 0.51       | short narrow notch                  |
| 19     | OD, axial                   | 5.0         | 0.4        | 0.63       | short narrow notch                  |
| 20     | OD, circumferential         | 5.0         | 0.2        | 0.17       | short shallow notch                 |
| 21     | OD, circumferential         | 5.5         | 0.4        | 0.29       | short notch                         |
| 22     | OD, circumferential         | 5.0         | 0.3        | 0.71       | short notch                         |
| 23     | ID, axial                   | 5.5         | 0.2        | 0.15       | short shallow notch                 |
| 24     | ID, circumferential         | 5.0         | 0.2        | 0.14       | short shallow notch                 |
| 25     | OD, oblique                 | 6.0         | 0.2        | 0.16       | short shallow notch                 |
| 26     | OD, oblique                 | 6.0         | 0.2        | 0.15       | short shallow notch                 |



OD short axial slot



OD short circumferential slot



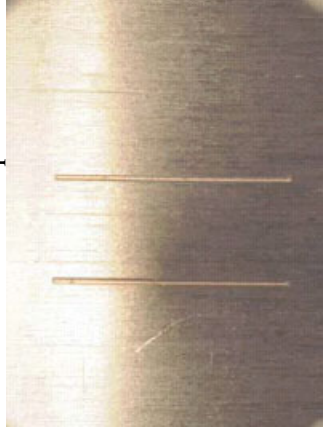
OD short oblique slot



OD short oblique slot



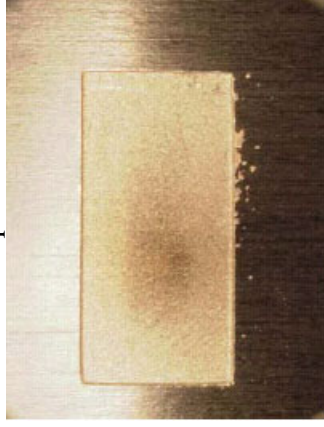
OD long axial slot



Two parallel OD circumferential slots



OD cross-like indication



OD rectangular indication

FIG. 7. Photographs of some of the OD features machined in the CH11 sample.

### 2.1.6. Canadian samples (CAN1 and CAN2)

The details of flaws in CAN1/2 samples with respect to their location, orientation, size and characteristics are given in Table 6 and Table 7.

Table 6. Flaw details in CAN1 sample

| Flaw # | Location | Length <sup>1</sup><br>(mm) | Width <sup>2</sup><br>(mm) | Depth <sup>3</sup><br>(mm) | Characterization  |
|--------|----------|-----------------------------|----------------------------|----------------------------|---|
| E1     | OD       | 1.07                        | 0.22                       | 0.124                      | axial DHC (semi-elliptical)   |
| E2     | OD       | 1.05                        | 0.199                      | 0.28                       | axial DHC (semi-elliptical)   |
| E3     | OD       | 1.98                        | 0.214                      | 0.125                      | axial DHC (semi-elliptical)   |
| E4     | OD       | 2.05                        | 0.204                      | 0.27                       | axial DHC (semi-elliptical)   |
|        |          |                             |                            |                            |   |
| F1     | OD       | 0.163                       | 1.1                        | 0.125                      | circumferential DHC (semi-elliptical)   |
| F2     | OD       | 0.157                       | 1.06                       | 0.265                      | circumferential DHC (semi-elliptical)   |
| F3     | OD       | 0.148                       | 1.94                       | 0.12                       | circumferential DHC (semi-elliptical)   |
| F4     | OD       | 0.146                       | 2.04                       | 0.27                       | circumferential DHC (semi-elliptical)   |
|        |          |                             |                            |                            |   |
| C1     | ID       | 3.32                        | 3.24                       | ~1.42                      | complex ~axial debris fret of 3 depths  |
| C2     | ID       | 3.9                         | 2.15                       | 0.995<br>0.83 <sup>4</sup> | simple axial debris fret with axial DHC (semi-elliptical)                               |
| C3     | ID       | >3.2                        | 3.3                        | 1.49<br>1.49               | complex ~axial debris fret with axial DHC (semi-elliptical)                             |
| C4     | ID       | 4.04                        | 2.14                       | ~0.78                      | simple axial debris fret  |
|        |          |                             |                            |                            |   |
| D1     | ID       | 2.3                         | 1.7                        | 0.47                       | circumferentially-oriented undercut simple debris fret                                  |
| D2     | ID       | 1.7                         | 2.3                        | ~0.85<br>0.73              | axially-oriented undercut simple debris fret with axial DHC (semi-elliptical)           |
| D3     | ID       | 1.64                        | 2.3                        | 0.71                       | axially-oriented undercut simple debris fret  |
| D4     | ID       | 2.3                         | 1.83                       | ~0.85<br>0.68              | circumferentially-oriented undercut simple debris fret with axial DHC (semi-elliptical) |
|        |          |                             |                            |                            |   |
| J1     | OD       | 19.5                        | ~0.1                       | ~0.08                      | axial installation scratch  |

<sup>1</sup> Length = Axial Extent.

<sup>2</sup> Width = Circumferential Extent.

<sup>3</sup> Depth = Through-Wall Extent.

<sup>4</sup> First entry is total through-wall extent, with DHC. Second entry is through-wall extent without DHC.

Table 7. Flaw details in CAN2 sample

| Flaw # | Inside/Outside | Length (mm) | Width (mm) | Depth (mm)                           | Characterization   |
|--------|----------------|-------------|------------|--------------------------------------|--|
| C1     | OD             | 1.93        | 0.18       | 0.31                                 | axial DHC (semi-elliptical)  |
| B1     | ID             | 12.4        | 3.25       | 0.23                                 | simple bearing pad fret  |
| B2     | ID             | 14.4        | 4.65       | 0.249 <sup>5</sup><br>0.152          | double overlapping bearing pad frets   |
| B3     | ID             | 12.4        | 3.32       | 0.428<br>0.251                       | simple bearing pad fret with angled DHC (semi-elliptical) in corner              |
| B4     | ID             | 14.3        | 4.72       | 0.426 <sup>6</sup><br>0.249<br>0.145 | double overlapping bearing pad frets with angled DHC (semi-elliptical) in corner |

Flaw truth was obtained by profilometry. Figure 8 shows photographs of some of the OD and ID flaws present in the CAN1/2 samples.

<sup>5</sup> First depth is deepest fret. Second depth is shallower fret.

<sup>6</sup> First = deepest point. Second = deepest fret depth without DHC. Third = depth of shallower fret.



OD axial calibration slot



OD axial DHC



Complex axial debris fret with axial DHC



OD circumferential calibration slot



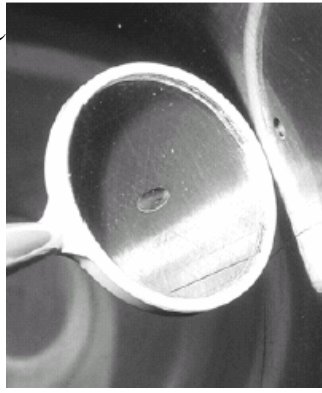
OD circumferential DHC



Single bearing pad fret



Normal beam calibration slot (15%)



Axial debris fret with axial DHC



Double overlapping bearing pad frets

FIG. 8. Photographs of some of the OD and ID features machined in the CANI/2 samples.

## **2.2. Inspection and diagnostics techniques**

### **2.2.1. Argentina**

Argentina used UT examinations for detection, location and characterization of flaws in the various PT samples. The shear wave pulse echo technique was employed using four shear wave transducers, two (in opposite directions) in the axial direction more sensitive to circumferential indications and two (in opposite directions) in the circumferential direction more sensitive to axial indications. The four reference notches from the Canadian Standard (ID axial, ID circumferential, OD axial and OD circumferential) were used for calibration and setting of the detection level.

The equipment used was a NEUS 8.80 Multichannel UT instrument. The UT transducers used were four 10 MHz, 38 mm focus, 0.250" diameter. The reference sensitivity was set according to the Canadian Standard.

### **2.2.2. India**

India primarily employed UT examination for detection, location and characterization of flaws in the PT samples. For some of the samples, ET was also employed for detection of ID flaws.

The inspection head comprises six UT transducers, four angle beam and two normal beam. The angle beam transducers are used in pairs, one looking axially and the other circumferentially. These are positioned in such a way that the beam from one transducer reaches the other after travelling two skip distances in the PT. For normal beam scanning, one of the transducers was focused on the OD, while the other was focused on the ID.

The PT samples were also examined by ET using a separate inspection head. ET was performed to detect the ID flaws. The curvature of the transducer was modified to match the inside surface of the PT and reduce the effect of lift-off variations. The probe wobbling signal is set horizontal by phase adjustment in the equipment. The amplitude of signal and its phase for ID flaws were recorded.

#### **2.2.2.1. UT techniques for flaw detection**

The following UT techniques were employed for detection of flaws in PTs during the CRP:

- Angle beam pulse-echo in axial direction (reflection mode);
- Angle beam pulse-echo in circumferential direction (reflection mode);
- Amplitude drop monitoring during angle beam pitch-catch in axial direction (transmission mode);
- Amplitude drop monitoring during angle beam pitch-catch in circumferential direction (transmission mode);
- Amplitude drop monitoring during normal beam examination using 10 MHz transducer focused on OD of PT.

#### **2.2.2.2. Specifications of UT and ET sensors**

All the UT transducers used during the examination are spherically focused. The specifications for these transducers and the ET sensor for different types of examination are given below:

- UT angle beam, axial and circumferential scan: 10 MHz, 10 mm diameter, 30 mm focal length;
- UT normal beam OD scan: 10 MHz, 6 mm diameter, 25 mm focal length;
- UT normal beam ID scan: 20 MHz, 6 mm diameter, 12 mm focal length;
- ET self-comparison differential coil, 300 kHz.

#### 2.2.2.3. *Reference sensitivity set-up*

Prior to examination of PT samples, the reference sensitivity for angle beam examination is set using reference notches. These notches are machined on a separate PT sample on ID and OD surfaces in axial and circumferential directions. The notches are 6 mm long, 0.2 mm wide and 0.15 mm deep. For normal beam examination, scanning sensitivity is set by adjusting the first backwall signal to approximately 80% of full screen height (FSH). For pitch-catch amplitude monitoring, the transmitted signal was set to approximately 80% FSH.

#### 2.2.2.4. *Scanning sensitivity*

For angle beam pulse-echo examination, scanning was carried out at 12dB above the reference. For normal beam and angle beam pitch-catch, scanning was carried out at the reference sensitivity.

#### 2.2.2.5. *Recording*

For angle beam pulse-echo scans, any indication exceeding 6dB over noise at the scanning sensitivity (generally, 20% FSH) is evaluated for recording and reporting. This criterion corresponds to a lower recording level (more stringent) than the recording criteria of 20% of reference level.

For normal beam scans, any drop in the amplitude of backwall signal by more than 5 to 10% of reference level is recorded.

For angle beam pitch-catch scans, any drop in the amplitude of transmitted signal by more than 5 to 10% of reference level is recorded. This scan provided a high degree of reliability for detection of flaws oriented unfavourably (oblique and tilted flaws).

#### 2.2.2.6. *NDE techniques for flaw sizing*

Once the flaw is detected and recorded, its length, width and depth are sized. The length and width of the flaws are determined using the 6dB drop technique using angle beam and normal beam signals. Following techniques are employed for assessing the depth of flaws:

- Time-of-flight in axial pitch-catch configuration;
- Time-of-flight in circumferential pitch-catch configuration;
- Time-of-flight using 10 MHz transducer for OD flaws;
- Time-of-flight using 25 MHz for ID flaws (surface profiling).

#### 2.2.2.7. *Data recording*

The data record for all the flaws included B-scan images and time-of-flight and amplitude plots. Figure 9 shows a B-scan image of a simulated DHC and a simulated debris fret.

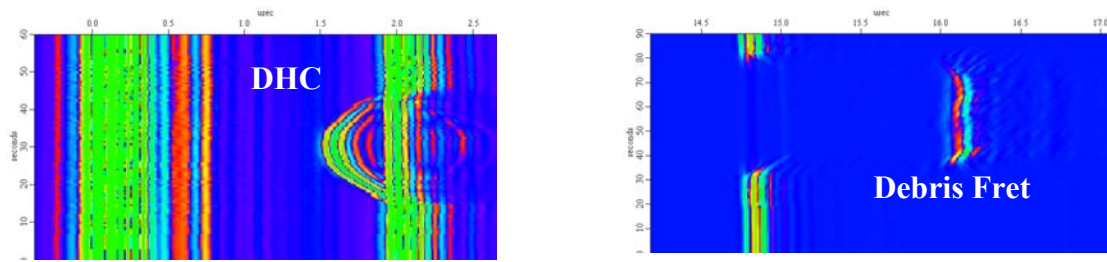


FIG. 9. B-scan images for simulated flaws.

### 2.2.3. Republic of Korea

Rep. of Korea employed an ET method for the detection and characterization of flaws in PT samples. The ET send-receiver transducer was designed to detect primarily ID flaws and attempt the detection of OD flaws; but this was known to be very challenging due to the penetration limitation of the magnetic field. This ET probe consists of two identical coils: one coil acts as a sender, and the other coil as a receiver. The transducer coil size is 3.5 mm OD, and it contains a ferrite core. For this inspection, 60 kHz was selected as the primary frequency to detect ID flaws and 20 kHz was chosen, as a second frequency, to attempt the detection of the OD flaws. 100 kHz was used as an additional frequency for confirmation. For signal analysis, A- and C-scan displays were used.

The calibration was performed using 20%, 50%, and 70% through wall notches. The recording criterion was set two times over the reference sensitivity. Any signals over reference level was recorded and evaluated. The correct flaw location was estimated using the encoder counts. The flaw length and width were sized by the 6dB drop technique. The flaw depth was estimated by measuring the phase angle of the signals.

### 2.2.4. Romania-NIRDTP

During this CRP, Romania-NIRDTP used an ET method for flaw detection and characterization. A new type of transducer, referred to as the RMF send-receive transducer was developed.

For the case of Zr-2.5% Nb ( $\mu=\mu_0=4\pi*10^{-7}$  H/m and  $\sigma=1.89*10^6$  S/m), with a frequency of 40 kHz, the standard depth of penetration is  $\delta = 1.83$  mm. The current density on the PT OD surface is ten times smaller than the density on the ID surface, still sufficient to detect material discontinuities on both PT surfaces and within the wall.

The RMF transducer is an ‘absolute’ send-receive type of transducer. The emission part is made from three rectangular coils  $120^\circ$  apart from each other, star connected and fed with a three-phased electrical current. The reception part is made of 24 identical coils arranged into a circumferential array. See Figure 10 for a photograph of the RMF send-receive transducer.

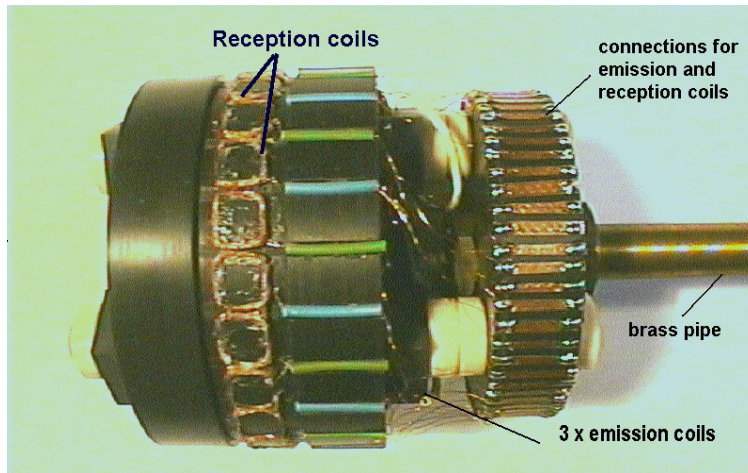


FIG. 10. Photograph of ET RMF send-receive transducer.

To use such transducer, special control equipment was designed and fabricated, comprising three programmable function generators type AWG 7223 with two outputs each supplying the alternative three-phased current system feeding the emission side of the transducer. The reception coils are sequentially interrogated, the signal being applied to the ET card, SFT6000N type, thus modified to accept an external reference. The interrogation is made using an analog multiplexer. The electronic boards were inserted into a PC. The signals delivered by the ET boards are stored in the computer memory and processed with a Matlab program. Figure 11 presents a schematic of this system.

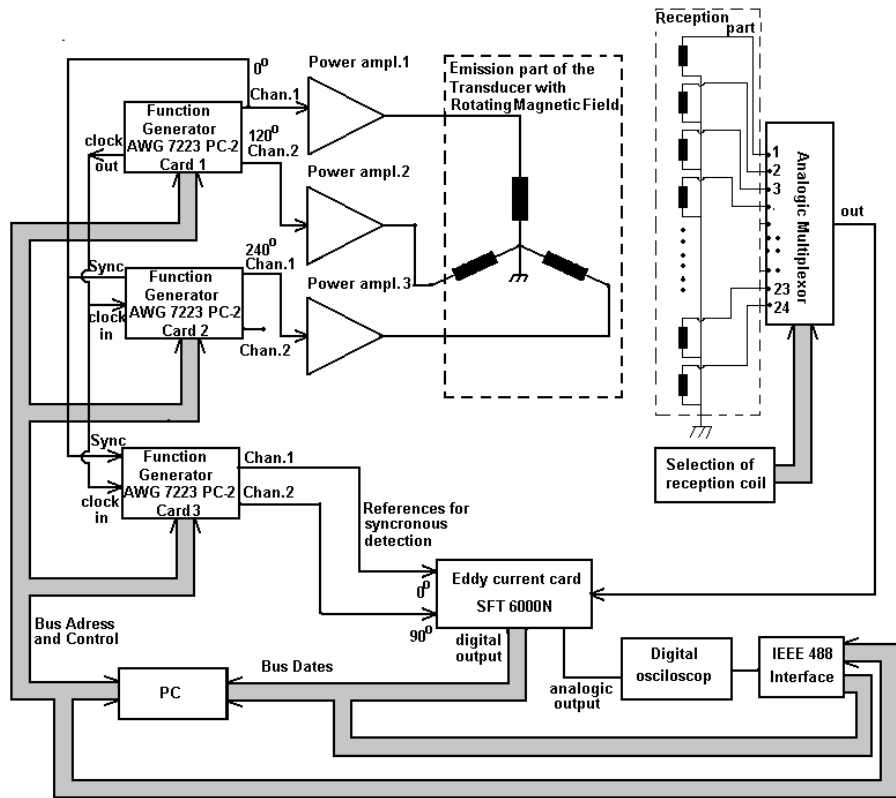
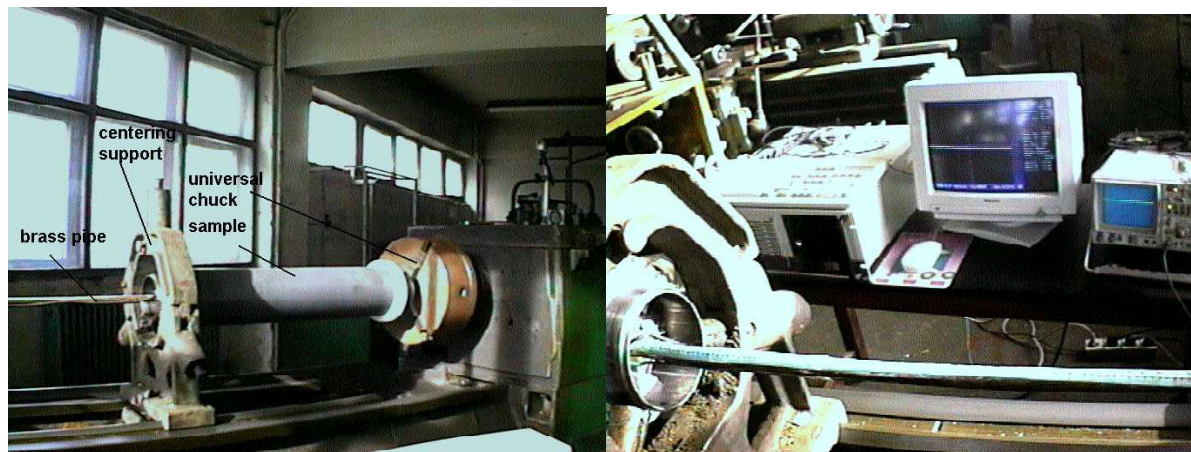


FIG. 11. Schematic of the ET inspection system fabricated at NIRDTP.

Due to the weight of the PT samples, they were mounted into an automatic chuck lathe. The transducers were automatically moved using 2 mm steps. Figure 12 presents a photograph of the experimental set-up.



*FIG. 12. Experimental set-up of the ET inspection system used at NIRDTP.*

During this CRP, theoretical aspects of the proposed transducer were studied using dyadic Green's functions and volume integral methods. The results of this work are presented in several publications [1–9], [13–16]. The model developed allows the solving of the forward problem to predict the response of the RMF transducer for different types of discontinuities, placed both on ID and OD surfaces of the PT [6]. At the same time, the inverse problem was solved to provide a method for evaluation of the geometrical shape and dimensions of the flaws from the response of the transducer [8].

The RMF send-receive transducer has shown very good detection capability for flaws situated on both ID and OD surfaces of the PT. The transducer's spatial resolution (minimum distance between two discontinuities distinctly distinguished) can be improved by the use of smaller reception coils. In the case of the RMF send-receive transducer, one reception coil covers approximately 15° of the PT circumference. It is thought that the use of many reception coils placed as an array improved the detectability. However, this complicates the hardware and software required and may result in a slower inspection speed.

The advantages of the RMF send –receive transducer used during this CRP are:

- detection of flaws both on the ID and OD surfaces
- good scanning speed

The drawbacks of this transducer are:

- poor spatial resolution due to large number of reception coils
- difficulty in data interpretation
- difficulty of precise assessment of circumferential position and orientation of flaws

#### **2.2.5. Romania-NNDT**

Thorough UT inspections were performed by Romania-NNDT on the various PT samples using the ISIS equipment developed at NNDT. The flaw detection and sizing methodology as well as other information are presented in detail on enclosed CD.

### 2.2.5.1. *Inspection equipment*

The ISIS-UT and ET system is a complex vertical laboratory system for simulating fuel channel inspections. The functional structure of ISIS-UT&ET integrates all applicable flaw detection and sizing UT and ET methods addressed by the Canadian Standard. This equipment consists of the following three main modules:

#### (1) ***Independent Scanning Inspection System (ISIS)***

It is a vertical high resolution scanning system that can be used for PT samples up to 750 mm in length. The maximum resolution of the system is 0.02 mm in the vertical direction and 0.01 mm in the circumferential direction.

#### (2) ***Multichannel UT and ET unit***

It consists of UT and ET instrumentation specific to each NDE function in a multichannel configuration. Depending on the NDE method or inspection requirements under testing, specific modular examination heads are used, with various transducer instrumentation or different interrogation geometry. Configuration of the UT multichannel system for flaw detection and sizing is as follows:

**Normal beam, high resolution – broadband examination.** This channel is based on the USIP 12/Krautkramer instrument; for UT spectral investigations, a Tektronix digital oscilloscope (100 MHz bandwidth, 1 GS/s sampling rate) is used.

**Standard “W” pitch-catch configuration for shear wave examination,** based on the multichannel KB 6000/Krautkramer instrument. Alternatively, a corresponding number of one-channel USIP 12/Krautkramer instruments can be used, as was the case in this CRP.

**UT dimensional measurements unit,** for measurement of the internal diameter and wall thickness of the PT sample.

**ET flaw detection and sizing** based on the dual frequency MIZ-17/ZETEC instrument.

#### (3) ***Command/Control and Data Acquisition/Processing unit (CC&DAP).***

The CC&DAP unit performs the real-time command and control of ISIS, the A/D conversion of the detected flaw signals, the synchronization of the entire system, and the data storage. It is also used for data analysis.

PT samples were examined during separate scans with adequate resolution using normal beam (longitudinal waves) and angle beam (shear waves) pulse-echo and pitch-catch configurations.

The transducers used are spherically focused 10 MHz nominal frequency, 6.35 mm effective diameter, and 35 mm focal distance. These transducers are used for both normal beam and shear wave examinations. Also, high-frequency normal beam examinations were performed with the polymer foil transducer (25 MHz nominal frequency, 25 mm focal distance, and a spot size of about 0.3 mm).

### 2.2.5.2. *PT samples scanning geometry*

Scanning of the PT samples was achieved by continuous rotation of the tube (on the circumferential axis) and translation of the inspection head along the axial direction. The tube rotation is in the counter-clockwise direction, so the UT indications coordinates are indexed

in the clockwise direction. The axial movement of the inspection head is performed going up in the sample under investigation.

#### 2.2.5.3. *Examination techniques*

A minimum of seven UT examinations was performed with the ISIS system to cover the requirements of the Canadian Standard. These are: normal beam – surface echo, normal beam – flaw echo, normal beam – back echo, pitch–catch (transmission) axial, pitch–catch (transmission) circumferential, shear waves (reflection) axial, shear waves (reflection) circumferential.

Regarding flaw detection, very good results were obtained with the axial and circumferential angle beam pitch-catch amplitude and time-of-flight monitoring, combined with high-resolution C-scan imaging. This technique enables determination of the flaw position (ID, OD, or within wall).

Romania-NNDT also used a 25 MHz normal beam broadband transducer focused on the OD with spectral analysis of the echo signals. This examination technique, based on Romania-NNDT research results [17], has proven to be very effective for sizing of flaws on the OD and within wall. UT based on spectral analysis is believed to have the potential to improve the flaw characterization and sizing capability in comparison with the “classical” broadband amplitude evaluation.

#### 2.2.5.4. *Flaw sizing methodology*

Dedicated software was developed and used as support for data analysis [18].

The 6dB drop technique using angle beam and normal beam was used to determine the position of a flaw and its length and width. Depth is the most important dimension when sizing flaws. Flaw depth is evaluated by the time-of-flight (TOF) images using normal beam. However, for flaws not necessarily small but having unfavourable orientation for normal beam reflection, flaw depth determination from the normal beam time-of-flight is not possible. In these cases, the shear wave amplitude comparison method is used. It consists of comparing the shear wave amplitudes of the flaw with a calibration feature of similar dimensions (known depth). Unfortunately, the flaw echo amplitude can be affected by many factors and, therefore, the corresponding depth estimate is not very accurate.

Romania-NNDT also applied the Time-Of-Flight Diffraction (TOFD) technique. This technique uses the modulation of the TOF versus flaw sound path generated by the interference of the elementary waves reflected on different surface elements of the flaw. The flaw depth is determined from the maximum variation  $\Delta$ TOF.

Flaw sizing was essentially based on the evaluation of the various C-scan images obtained during the different examinations. However, for each PT sample, a number of selected indications were re-evaluated by direct (stationary) signal analysis by optimal positioning on the flaw (especially for verification of the depth values of the near ID surface flaws).

## 2.2.6. *Canada*

### 2.2.6.1. *UT*

Two angle beam transducers are directed circumferentially, in order to detect and size axially oriented flaws, and two are directed axially, to detect and size circumferentially oriented flaws. In both cases the beams are in opposing directions because the orientation of flaws with respect to the surface can make them more or less reflective. Thus two beams in opposite directions makes sizing more reliable. Also, the beams are focused on the same point of the inner surface allowing pitch-catch B-scans used for depth sizing. Two normal beams are directed at the PT. One, the 10 MHz transducer, detects (and provides information for sizing) reflectors in the tube wall, such as laminar discontinuities or sub-surface voids, using a long-focus probe that sends acoustic energy across the tube wall, reflecting multiple times from the far surface. This probe is also useful for detecting volumetric flaws on either surface, which do not produce reliable shear wave signals. The second, the 20 MHz transducer, detects and sizes inside surface fretting, using a tightly focused probe that has good sensitivity to changes in the inside tube surface profile, but does not penetrate the full wall of the PT effectively.

Three scans are usually required in a typical inspection sequence. These are:

- Initial calibration check.
- Main scan of the sample.
- Final calibration check.

The simple three-step procedure given above is common to nearly all NDE, whether or not they involve UT methods, and makes the validity of the results unassailable under code requirements.

Data are recorded using a computer controlled data acquisition system. It takes the output from the flaw detector and digitises it through an analogue-to-digital converter, which is interfaced to the UT instrument. By collecting the data and assigning position to the signals, the data can be stored and displayed in any of the several formats preferred by the examiners. This is limited only by the capabilities of the display software.

The simplest method of displaying data for analysis for the purpose of detection is the strip chart format. This involves taking the gated peak detector output from the UT flaw detector, and assigning it to a channel on the computer that displays it against time on a chart. The C-scan display can also be produced. This presents the data in the form of a two dimensional map over the length and circumference of the PT. The C-scan is particularly useful for estimating the length and width of flaws and depth for large volumetric flaws using the 20 MHz probe. UT imaging techniques can be applied to help in the characterization of an indication. These may be performed in pulse-echo or pitch-catch, and usually generate a third method of data display known as a B-scan. The B-scan uses all the reflection versus time data of the transducer “shot”, at different adjacent locations of the tube, to create an UT cross-sectional view of the tube wall. The different reflective facets of the flaw can often be seen in this type of display. This is the primary tool for depth estimation. Figure 13 shows one of the inspection head with the UT cluster used for flaw detection and characterization.

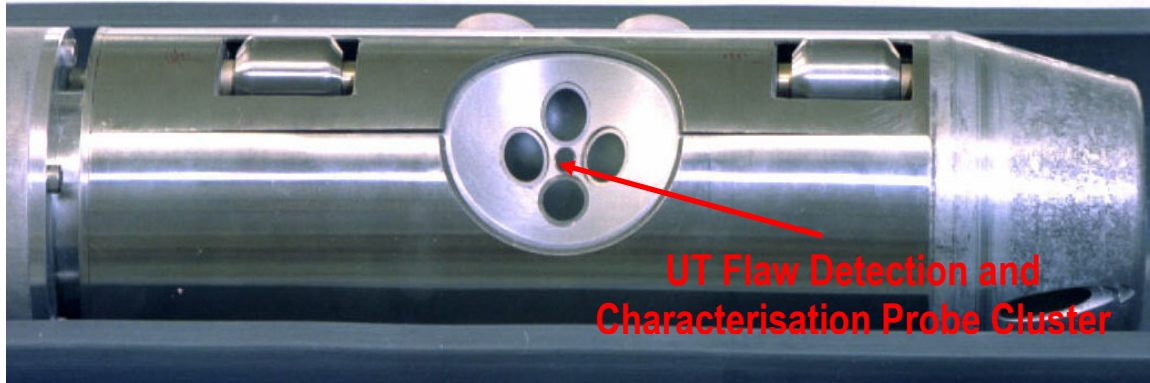


FIG. 13. UT cluster with the four shear wave probes and one normal beam probe at the centre; the 20 MHz probe is usually located 180° opposite to the normal beam probe (different heads with various configurations have been used for this project).

#### 2.2.6.2. ET

While CAN/CSA-N285.4-94 [10] specifically addresses UT inspection, ET inspection provides a complementary technique, decreasing the probability of missing significant flaws in PTs such as surface-breaking flaws with particular angular orientation or shape that may be missed by UT detection methods.

Two ET probes are used for detection and sizing: the G1 and the TDR probes. The G1 probe may be operated in the G1 (which is the differential mode) and absolute impedance modes. The details of coil arrangements are given in [11]. The G1 mode is predominantly used for detection and sizing. The lift-off is adjusted to generate a signal for near-surface flaws that is phase-rotated by up to 90° with respect to signals produced by lift-off variations. The usual operating frequency for the G1 mode is 100 kHz. Operation of the G1 mode at 50 kHz permits discrimination between flaws and ferromagnetic indications. The TDR probe consists of a single transmit and two receive coils that provide sensitivity in-line with the direction of scan and perpendicular to it. This allows for differentiation between narrow axially and circumferentially oriented indications.

Calibration before inspection of a fuel channel is used to verify system operation and record system sensitivity to reference discontinuities. Calibration and main scans are performed with the same helical spiral, typically at a 1 mm pitch. Data acquisition is time based at 1800 samples/s or 5 samples/deg. A final calibration verifies proper probe operation and that sensitivity of probe and instrument have not changed appreciably during the time of the scan.

Detection of PT flaws is based upon a threshold signal amplitude in the G1 mode at 100 kHz that is set at the maximum amplitude obtained from a nominally 0.25 mm deep, 6 mm long and 0.15 mm wide EDM notch calibrated to 1.0 volt. For in-service inspections, application of the threshold criterion for the detection of flaws requires consideration of various in-service factors that may produce signal amplitudes above the detection level. Some of these factors include the presence of ferromagnetic material, the presence of conducting materials other than the base material being examined, resistivity variations in the base material, local geometry changes, lift-off variations, the difference between tight flaws and those with large circumferential extent, orientation and indications with axial extent less than the resolution of the probe (typically 3 mm).

ET flaw detection is particularly sensitive to surface breaking indications on the inspection surface. Sizing estimates for narrow and long indications may be estimated from a comparison of signal amplitude with that obtained from notches in the calibration tube. Signal amplitude is largely proportional to the area with which the indication breaks the inner PT surface. Therefore, indication length and width are important parameters in accurately estimating depth. An additional factor to be taken into account when estimating flaw depth is that ET sensitivity decreases exponentially with the depth into the material. Accurate sizing depends largely on a known uniform extent and depth of a particular indication. Except for known modes of degradation, the majority of indications are expected to be non-uniform. Therefore accurate sizing estimates may not be obtainable without additional information from sources like UT, video, and replication concerning the specific shape, orientation, length and width of an indication. Figure 14 shows one of the inspection head with the G1 probe used for flaw detection and characterization.

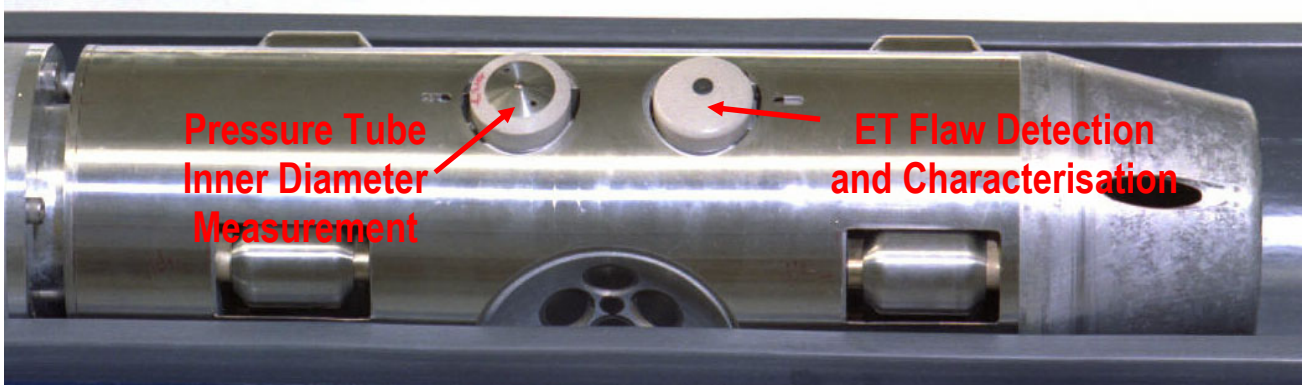


FIG. 14. The ET probe shown on the right is a G1 probe; the ET Transmit Dual Receive (TDR) probe is usually located 180° opposite to the G1 probe (different heads with various configurations have been used for this project).

#### 2.2.6.3. Profilometry

Impressions (replicas) of indications were taken in a similar way (similar technique and mold compound) as for in-service inspections. The positive and negative replicas were then examined by profilometry to provide full characterization of the indications.

### 2.3. Assessment of results

The sample summary reports contained an in-depth analysis of the results (multiple plots, tables, error estimates). This was very useful information in preparing the following concise assessment. The sample summary reports are available in the attached CD and can be consulted for detailed information. This information was consolidated to identify the best techniques for detection and sizing during this assessment as follows.

- For flaw detection, location and orientation: a simple yes/no criterion was used: was the flaw detected, properly located and its orientation correctly determined? If so the technique was evaluated to be appropriate.
- The assessment of flaw sizing was based upon comparison of NDE flaw sizing estimates with the true value leading to the identification of the best techniques for the different types of flaws.

During this CRP, the participating laboratories were required to detect flaws, locate them with respect to the reference punch mark, report their orientation, provide sizing estimates for

length, width and depth and characterize them per type such as debris fret, DHC, lap type. This section provides an assessment of the performance of each participating laboratory for each of these tasks. Furthermore the individual techniques are evaluated with respect to their detection and sizing capabilities.

### **2.3.1. Flaw location**

Flaw location refers to axial and rotary positions and position of the flaw in the wall (ID, OD and within wall). Most NDE methods were accurate in this regard, hence, no further analysis will be provided in this report.

### **2.3.2. Flaw orientation**

Flaw orientation can be axial, circumferential, oblique (at an angle to the tube axis) and tilted (in the radial direction). Most of the flaws have been reported with the correct orientation. It was nearly perfect for the flaws oriented either axially or circumferentially. For oblique and tilted orientations, the estimation was less accurate. Four laboratories reported consistently correct angles of inclination (oblique and tilted): Argentina, Canada, India and Romania-NNDT. Romania-NIRDTP and Rep. of Korea had more difficulty. From the NDE techniques employed by each country and the flaw type in question, it can be concluded that C-scan imaging using normal beam backwall drop, normal beam flaw echo monitoring and angle beam shear wave are the most suitable techniques for assessing the flaw orientation angle.

### **2.3.3. Flaw detection and sizing**

With respect to flaw detection and sizing it was observed that due to the use of a combination of techniques India, Romania-NNDT and Canada performed very well. Considering that only one technique was used, namely ET send-receive probe with Rotating Magnetic Field, and therefore no comparison could be done between different estimates, Romania-NIRDTP also did very well, especially in detecting the OD flaws. Those flaws are known to be a challenge due to the penetration limitation of ET. Romania-NIRDTP did miss few flaws and provided overall slightly less accurate estimates, which once again can be directly attributed to the use of a single technique. Argentina performed well in terms of detection and length sizing but does not have yet a depth sizing capability. Rep. of Korea used an ET send-receive probe known to have penetration limitation, which limits detection of OD flaws but it worked fairly well to detect and size ID flaws.

#### **2.3.3.1. NDE methods for flaw detection**

Argentina, India and Romania-NNDT employed only UT, while Rep. of Korea and Romania-NIRDTP employed only ET for flaw detection. Canada employed, as for their in-service inspection both UT and ET, even though ET is limited to the ID flaws.

#### **UT for flaw detection**

The detectability of flaws by UT was found to be equally reliable for ID and OD flaws.

Participating laboratories used different UT techniques. The effectiveness of the different UT techniques for detection of various types of flaws is summarized in Table 8.

Table 8. Effectiveness of UT techniques for flaw detection

| Technique   | Employed by                                  | Type of Flaw              | Flaw Detection Capability         |
|---|--|---------------------------|-----------------------------------|
| angle beam shear wave pulse-echo  | Argentina<br>Canada<br>India<br>Romania–NNDT | axial and circumferential | very good                         |
|   |  | oblique and tilted        | poor                              |
|   |  | lap-type or laminar       | poor                              |
|   |  | smooth debris fret        | poor                              |
| angle beam shear wave pitch-catch: amplitude drop and time-of-flight monitoring | India<br>Romania-NNDT                        | axial and circumferential | good, but inferior to pulse-echo  |
|   |  | oblique and tilted        | very good                         |
|   |  | lap-type or laminar       | very good                         |
|   |  | smooth debris fret        | good                              |
| normal beam backwall drop   | Canada<br>India<br>Romania–NNDT              | axial and circumferential | good, but inferior to pulse-echo  |
|   |  | oblique and tilted        | good, but inferior to pitch-catch |
|   |  | lap-type or laminar       | very good                         |
|   |  | smooth debris fret        | very good                         |
| surface profiling (only for ID flaws)   | Romania–NNDT                                 | axial and circumferential | good, but inferior to pulse-echo  |
|   |  | oblique and tilted        | good, but inferior to pitch-catch |
|   |  | lap-type or laminar       | not applicable                    |
|   |  | smooth debris fret        | very good                         |

Based on the results analysis, the ‘Best’ and complementary UT techniques for detection of various types of flaws in PTs are presented in Table 9.

Table 9. Best and complementary UT techniques for flaw detection

| Type of Flaw   | Technique <sup>7</sup>   |
|--|--|
| axial and circumferential ID or OD                     | conventional shear wave pulse-echo<br>amplitude drop monitoring with angle beam<br>pitch-catch and normal beam |
| oblique and tilted on ID and OD                        | amplitude drop monitoring with angle beam<br>pitch-catch<br><br>normal beam backwall drop                      |
| lap-type or laminar                                    | normal beam backwall drop<br><br>time-of-flight monitoring with angle beam<br>pitch-catch                      |
| fretting damage on ID due to debris<br>and bearing pad | surface profiling<br><br>normal beam backwall drop   |

***ET for flaw detection***

Romania-NIRDTP showed a good detectability of both ID and OD flaws even though higher for ID than for OD. Three types of transducers were used during this CRP. The effectiveness of each for detection of various types of flaws is given in Table 10.

Based on the results analysis, the ‘Best’ and complementary ET techniques for detection of various types of flaws in PTs are presented in Table 11.

---

<sup>7</sup> First technique shown is the best and the second is complementary.

Table 10. Effectiveness of ET technique for flaw detection

| <b>Probe Design</b>    | <b>Employed by</b> | <b>Type of Flaw</b>          | <b>Flaw Detection Capability</b> |
|------------------------|--------------------|------------------------------|----------------------------------|
| RMF send-receive probe | Romania-NIRDTP     | OD axial and circumferential | good                             |
|                        |                    | ID axial and circumferential | good                             |
|                        |                    | lap-type or laminar near OD  | good                             |
|                        |                    | debris fret on ID            | poor                             |
|                        |                    | bearing pad fret on ID       | good                             |
| surface probe          | Canada             | OD axial and circumferential | not applicable                   |
|                        |                    | ID axial and circumferential | good                             |
|                        |                    | lap-type or laminar near OD  | not applicable                   |
|                        |                    | debris fret on ID            | very good                        |
|                        |                    | bearing pad fret on ID       | very good                        |
| send-receiver          | Rep. of Korea      | OD axial and circumferential | not applicable                   |
|                        |                    | ID axial and circumferential | poor                             |
|                        |                    | lap-type or laminar near OD  | not applicable                   |
|                        |                    | debris fret on ID            | poor                             |
|                        |                    | bearing pad fret on ID       | good                             |

Table 11. ‘Best’ ET techniques for flaw detection

| Type of Flaw                    | Technique  |
|---------------------------------|--|
| OD, irrespective of orientation | RMF send-receive probe   |
| ID, irrespective of orientation | RMF send-receive probe<br>surface probe                        |
| lap-type or laminar             | RMF send-receive probe   |
| debris frets                    | surface probe  |
| bearing pad frets               | RMF send-receive probe<br>surface probe<br>send-receiver probe |

2.3.3.2. *NDE methods for flaw sizing*

With flaws separated into three types (axial and circumferential ID or OD, oblique ID or OD and fretting damage on ID), it can be concluded that the depth sizing accuracy can be ranked as follows (better to worst): fretting damages on ID, axial and circumferential ID or OD and then oblique ID or OD. Depth sizing of lap-type or laminar flaws is not of interest, although they are required to be reliably detected irrespective of their location within the PT wall. Undercut flaws were found to be challenging and their depths were generally undersized. Table 12 presents the best techniques categorized by flaw types to size length, width and depth.

Table 12. Best UT and ET techniques for flaw sizing

| Type of Flaw                       | Techniques for Flaw Sizing  |   |  |
|------------------------------------|---|---|--|
|                                    | Length  | Width   | Depth  |
| axial and circumferential ID or OD | 6dB drop using angle beam and normal beam for OD flaws<br><br>UT surface profiling using 20/25 MHz for ID flaws | ET RMF send-receive for OD flaws<br><br>UT surface profiling using 20/25 MHz for ID flaws | time-of-flight in pitch-catch mode<br><br>time-of-flight using normal beam<br><br>UT surface profiling using 20/25 MHz for ID flaws<br><br>ET surface probe for ID flaws |
| oblique and tilted                 | UT C-scan image using normal beam   | ET RMF send-receive probe   | time-of-flight in pitch-catch mode<br><br>time-of-flight using normal beam<br><br>UT surface profiling using 20/25 MHz for ID flaws<br><br>ET surface probe for ID flaws |
| lap-type or laminar                | UT C-scan image using normal beam   | UT C-scan image using normal beam   | time-of-flight using normal beam   |
| fretting damage                    | UT surface profiling using 20/25 MHz transducer   | UT surface profiling using 20/25 MHz transducer   | UT surface profiling using 20/25 MHz transducer<br><br>ET surface probe for ID flaws   |

#### 2.3.4. Flaw characterization

This criterion of performance assessment is directly linked to sizing accuracy. Those that have good results with sizing have usually better data for reporting the type of flaw (debris fret, DHC, lap-type). This is also dependent on the experience with in-service inspections. It was observed that all participating laboratories did fairly well in regard to this criterion.

### 3. DISCUSSION OF RESULTS

In the assessment section, the results were presented as best techniques for detection and best techniques for sizing for each type of flaw. This section will attempt to be more practical in that it tries to answer the question “which techniques need to be implemented on an in-service inspection tool, in order to attain reliable detection and accurate sizing?”

Tables 9 to 12 can be summarized as follows when considering all types of flaws. For detection of axial and circumferential flaws the angle beam pulse-echo technique is good enough. However, the amplitude drop using pitch-catch technique is required for reliable detection of flaws with unfavourable orientation (oblique and tilted flaws). For laminar or lap-type flaws, the normal beam backwall drop technique is most effective. This technique also works fairly well for fretting damage, although UT surface profiling at high frequency is also highly reliable. With respect to the sizing, surface profiling using high frequency probes (20/25 MHz) often gives the best results for length, width and depth for ID flaws. Because of the tightness of the beam, the 20dB drop technique is the most appropriate when sizing length and width. For length and width determination of all OD flaws, irrespective of orientation angle, backwall echo monitoring (C-scan image) using 6dB drop with normal beam is the most accurate technique. 6dB drop using angle beam pulse echo can also be useful for length estimation of axial and circumferential flaws, but not for the oblique ones. For depth determination of all flaws (ID and OD), time-of-flight with normal beam and angle beam pitch-catch give very good results.

Canada has reported in a publication [12] that ET can be complementary to UT by providing an independent set of results and therefore increase confidence in detection and sizing accuracy. ET is inherently a very sensitive technique to surface breaking flaws on the ID, and that characteristic was observed once again in this CRP. The ET send-receive probe with Rotating Magnetic Field used by Romania-NIRDTP showed excellent results for detection of flaws on the OD, which is a remarkable achievement considering the penetration limitation of ET. The ET surface probes used by Canada gave consistently good depth estimates for the ID flaws; length and width estimates were not as good as UT estimates. However, the ID flaws represent a large majority of the flaws encountered in-service and the depth is in many regards the most critical dimension of the three (between length, width and depth) even though it is understood that the flaw is regarded as a whole when being dispositioned. The sizing provided by Romania-NIRDTP ET technique was also quite good (particularly for width which was recognized as a weakness for most other techniques) even though not as consistent but that can be directly attributed to the disadvantage of having only one technique in their arsenal. Rep. of Korea used a send-receiver probe that showed good results for ID flaws. Canada also used a transmit-dual receive probe that gave very satisfactory results. Such probes have better penetration than standard surface probes and allow accurate determination if a flaw is subsurface or when used as pairs (at 90° from each other) for determination of the angle of inclination. Further development work on this type of probes should continue.

Tables 13 and 14 summarize the above discussion.

Table 13. Recommended UT and ET detection techniques for all types of flaws

| Type of Flaw                       | UT                        | ET                     |
|------------------------------------|---------------------------|------------------------|
| axial or circumferential, ID or OD | angle beam pulse-echo     | RMF send-receive probe |
| oblique or tilted, ID or OD        | angle beam pitch-catch    | RMF send-receive probe |
| lap-type or laminar                | normal beam backwall drop | RMF send-receive probe |
| fretting damage                    | UT surface profiling      | surface probe          |

Table 14. Recommended UT and ET sizing techniques for all types of flaws

| Length   | Width  | Depth  |
|--|--|--|
| UT surface profiling using high frequency (20/25 MHz) for ID flaws   | UT surface profiling using high frequency (20/25 MHz) for ID flaws | UT surface profiling using high frequency (20/25 MHz) for ID flaws |
| normal beam C-scan image using 6dB drop for OD flaws and flaws within wall, and angle beam pulse-echo for axial and circumferential OD flaws | 6dB drop using normal beam for OD flaws and flaws within wall      | ET surface probe for ID flaws                                      |
|  | ET RMF send-receive probe for all flaws                            | time-of-flight in pitch-catch mode for all flaws                   |
|  |  | time-of-flight using normal beam for OD and flaws within wall      |

## 4. CONCLUSIONS AND RECOMMENDATIONS

### 4.1. Conclusions

In a series of blind tests on prepared samples of pressure tubes with intentional flaws, essentially all flaws, of a serious nature, as well as flaws of less concern, were detected. This conclusion applies to most of the participating institutes, using different methodologies. Regardless of the location, the axial and circumferential flaws and flaws resulting from fretting were detected with high reliability. Oblique flaws, which are more challenging to detect, were nearly always detected. For such flaws, a new approach, used for the first time in this CRP, based on monitoring the amplitude drop and time-of-flight during UT angle beam pitch-catch was proven to be very effective for detection.

All flaw locations were reported correctly.

The orientations of all axial and circumferential flaws were reported correctly. The orientation of oblique flaws was challenging but correctly reported in most cases.

NDE sizing of length and depth for axial and circumferential flaws and sizing of length, width and depth for flaws resulting from fretting were estimated close to their real dimensions. Sizing of oblique flaws was fairly accurate as well. The depth sizing of flat-bottom reflectors was not very accurate. They represent lamination or lap-type flaws. Since such flaws could not be generated in PT samples, they were simulated by flat-bottom reflectors drilled from the OD surface. In real conditions, depth sizing of lamination type of flaws is not an issue. Hence inaccurate estimation of depth for flat-bottom reflectors observed in few cases is not a cause of concern. Width sizing accuracy was poor for the fine notches, irrespective of their orientation and location. The high-frequency broadband normal beam technique was useful for characterization of OD flaws and flaws within wall.

This CRP has recommended a set of NDE techniques (UT and ET) for detection and sizing of all types of flaws during in-service inspection of PTs. UT was proven to be highly effective for the majority of the flaws. The good performance of ET is to be noted particularly to size ID flaws (surface probe) and to detect OD flaws (ET send-receive probe with Rotating Magnetic Field) even though further development is required.

### 4.2. Recommendations

Some inspection and diagnostic methods performed better than others in detecting and sizing the flaws. Table 13 and Table 14 show the recommended set of NDE techniques for detection and sizing of flaws respectively. However, it was observed that no NDE technique could accurately estimate the width of the fine notches. Conventional approaches like amplitude comparison with reference flaw and new approach like C-scan imaging were used to evaluate the width of very fine flaws. However, none of these approaches could yield satisfactory results. The tip radius of the flaw is the important parameter; its value reflects if the flaw is sharp enough to initiate DHC or blunt enough to remain dormant and harmless throughout the life of the PT. Although replication is a useful tool in this regard, only Canada has developed it for use in reactor. Hence, development of a reliable NDE method based on UT and ET for accurate estimation of flaw width is desirable.

It was noted that characterization of a flat-bottom reflector near the ID was challenging. It is therefore recommended to improve the near surface resolution of the normal beam examination to reliably detect lamination or lap-type flaw near the ID surface.

Depth sizing using surface profiling could be underestimated in cases where the flaws are tight, not allowing much access for the UT beam through the mouth opening, or when the flaw is tilted. It is recommended to further refine the angle beam pitch-catch technique for depth sizing of such flaws. It may be required to have different sets of UT transducers for sizing OD and ID flaws.

Use of high-frequency broadband transducers combined with spectral analysis should be evaluated as a way for improving flaw characterization.

The development of methodologies for uncertainty estimates in NDE flaw sizing should be explored.

Use of ET as a complementary technique to UT is recommended because of the inherent strengths and weaknesses of each technique. ET showed some very satisfactory results and is particularly sensitive to some flaws that UT may not detect as well (gradual and shallow indications). Data fusion of UT, ET and visual examination can improve the reliability and accuracy of inspection results for PTs. It is therefore necessary to investigate its usefulness for PT inspection and diagnostics.

This collaboration has confirmed the good performance of inspection and diagnostics NDE techniques using PT samples with artificial flaws. A logical next step would be to carry out a similar exercise with PT samples with real flaws.

An international collaboration to address the above recommendations would be quite effective.



## APPENDIX I. GLOSSARY

### I.1. Ultrasonic testing terminology

**Angle beam pulse-echo:** This technique, which uses the same transducer as transmitter and receiver, is based on monitoring the reflected signal from the flaw for its detection. The pressure tube examination involves two independent angle beam pulse-echo scans: axial and circumferential. During scanning, the ultrasonic beam travels along the axial or circumferential direction of pressure tube (generally at 45°) and gets reflected when it encounters a flaw. The reflected signal reaches back to the transducer, if the major dimension of the flaw is oriented perpendicular to the beam direction, i.e. axial flaw for circumferential scan and circumferential flaw for axial scan. If the flaw is oblique, the reflected signal from the flaw may not reach the transducer and the flaw will be missed.

**Angle beam pitch-catch:** This technique uses two transducer, one acting as a transmitter and the other receiver. For pressure tube examination two independent pairs are used, one looking axially and the other circumferentially. Each pair is mounted in such a way that the ultrasonic beam from the transmitter reaches the receiver after travelling two skip distance in the pressure tube. This configuration ensures that the ultrasonic beam gets disturbed by the flaw on ID and OD surface as well as within wall. During scanning, when the ultrasonic beam encounters a flaw, it gets reflected. This results in the drop in the amplitude of the signal at the receiver. By monitoring this amplitude drop one can find out the presence of flaw in pressure tube. This technique is highly reliable for detection of oblique and tilted flaws. One can also monitor the time-of-flight of the transmitted signal for flaw detection, especially for laminar flaws.

**Normal beam backwall drop:** This technique used a normal beam transducer for detection of flaws in pressure tube. The backwall signal from pressure tube OD is adjusted to pre-determined height. During scanning, when the ultrasonic beam encounters a flaw, a part of it gets reflected. This results in drop in the amplitude of the backwall echo signal. One can also monitor the amplitude of the flaw signal or time-of-flight of the backwall signal to detect flaw using normal beam. This technique can detect flaws in all orientations across the entire thickness of the pressure tube.

**Surface profiling:** This technique uses a high frequency (20 - 25 MHz) normal beam transducer, sharply focused on the ID of the pressure tube. When the ultrasonic beam encounters a flaw, there is a change in the amplitude and time-of-flight of the interface (water to zirconium alloy) signal. This technique is very effective for detection and sizing of ID flaws in pressure tube.

**B-scan image:** Two dimensional representation of the flaw echo amplitude against time - of - flight and one of the transducer coordinate during scanning;

**C-scan image:** Two dimensional representation of the flaw echo amplitude or time - of - flight against two of the transducer coordinates during scanning;

**6 dB / 20 dB drop technique:** This technique is used for finding the length of the flaw using angle beam pulse-echo technique. The reflected signal from the flaw is maximized and then transducer is moved along the major dimension of the flaw in either direction from the point of maxima, till the amplitude of the reflected signal falls to 50 % (6 dB) of its maximum

value. The distance between the two points on either side of the maxima gives the flaw length. In the 20 dB drop technique, the amplitude of the reflected signal is allowed to fall to 10 % of maximum. The 6 dB drop technique can also be used with normal beam, where the length of the flaw can be found out from C-scan image based on flaw signal or backwall signal;

**Time-of-flight techniques for depth sizing:** In conventional pulse-echo technique, the depth of the flaw is found out by comparing the amplitude of reflected signal from the flaw with that from the reference notch. However since the reflected signal from flaw is adversely affected by flaw orientation, surface roughness, transparency. etc., this technique tends to undersize real flaw. The time-of-flight (TOF) based techniques are based on monitoring the time-of-travel of the diffracted signal from the flaw tip. Since the TOF is dependent on the flaw depth alone, the sizing accuracy achieved by this technique is excellent. TOF based depth sizing technique can be used during normal beam as well as angle beam pitch-catch scan.

## I.2. Eddy current testing terminology

**Absolute Measurement** - A Measurement made without a direct reference to a second signal or measurement.

**Acceptance Standard** - A controlled specimen containing natural or artificial discontinuities that are well defined and similar to the maximum acceptable discontinuity, in size and extent, in the product.

- Also may refer to the document defining acceptable discontinuity size limits.

**Amplifier** - A device to increase or amplify electric impulses.

**Amplitude** - (1) The maximum absolute value obtained by the disturbance of a wave or any quantity that varies periodically. (2) The vertical height of a received signal on an A-scan. It is measured from peak to peak for an RF presentation or from base to peak for a video presentation.

**Angular Frequency** - For any oscillation, the number of vibrations per unit time, multiplied by  $2\pi$ . Also known as angular velocity and radian frequency.

**Area-Amplitude Blocks** - Calibration blocks in which there are a series of flat-bottomed holes of varying diameter.

**Array Transducer** - A transducer made up of several individually piezoelectric elements connected so that the signals they transmit or receive may be treated separately or combined as desired.

**Artifact** - In non-destructive inspection, an indication that may be interpreted.

**Artificial Discontinuity** - A feature, such as a notch, hole or crack, that is manufactured to closely resemble a natural defect.

**Attenuation** - The reduction in the level of a quantity, such as the intensity of a wave or radiation.

**Axial** - Longitudinal or parallel to the axis or centerline of a part.

**Background Noise** - The extraneous signals caused by random signal sources within or exterior to the ultrasonic testing system, including the test material. Sometimes called grass or hash.

**Bobbin** - A cylinder, cone or reel holding thread or yarn

**Boundary** - The edge, end or face of a finite medium.

**Calibration** - The process whereby the magnitude of the output of a measuring instrument is related to the magnitude of the input force driving the instrument (i.e. Adjusting a weight scale to zero when there is nothing on it).

**Capacitance** - The property of an electrical circuit that opposing a change in voltage. Capacitance enables devices or circuits to hold an electrical charge.

**Capacitive Reactance** - The opposition to alternating current due to the capacitance of a capacitor, cable, or circuit.

**Characteristic Frequency Ratio** - It allows the test coil operating point to be specified in terms of a single quantity rather than four independent variables.

**Circuit** - A closed path followed or capable of being followed by an electric current.

**Circuit Diagrams** - A type of diagram that is a pictorial way of showing circuits.

**Circumferential** - Around the circumference, or periphery, of circular or cylindrical object. Also called tangential or hoop when referring to stresses.

**Circumferential Coil** - See encircling and internal probes.

**Coil** - More than one loop of a conductor wound in a spiral. Also called a solenoid.

**Comparative Test Block** - A metal block specially cracked and having two separate, but adjacent areas for the application of different penetrants so that a direct comparison can be obtain.

**Compensator** - An electrical matching network to compensate for electrical impedance differences.

**Complex Electrical Impedance** - In a typical AC circuit, resistance  $R$  and reactance  $X$  combine in vector fashion to form a complex impedance. Reactance is conventionally multiplied by the positive square root of  $-1$  ( $j$ ), to express  $Z$  as a complex number of the form  $R + jX$ .

**Composite** - A product that is produced by combining several different material products to arrive at desired set of properties. Fiber glass, carbon graphite epoxy, and carbon fiber are examples of composite material.

**Conductivity** - A measure of the ability of a material to conduct electrical current.

**Conductors** - Materials that have free electrons and allow electrical current to flow easily.

**Controlled Area** - A defined area in which the occupational exposure of personnel to radiation or to radioactive material is under the supervision of the individual in charge.

**Coupon** - A piece of metal from which a test specimen is to be prepared. Often an extra piece that is cut from a casting or forging.

**Crack** - A long narrow discontinuity

**Crack Growth Rate** - The change in crack length per number of fatigue cycles.

**Current (I)** - The flow of electrons. Measured in amperes.

**Current Density** - Current divided by the electrode area (current per unit area of the electrode)

**Cutoff Frequency** - A point or level marking a designated limit ; a sudden drop in amplification or responsiveness of an electric device at a certain frequency

**Cycle (Hertz)** - One complete set of recurrent values of a periodic quantity comprises a cycle.

**Damping** - Limiting the duration or decreasing the amplitude of vibrations.

**Defect** - A discontinuity or other imperfection causing a reduction in the quality of a material or component.

**Delamination** - A laminar discontinuity such as an area of unbonded materials.

**Depth of Penetration (Standard)** - The depth to which the eddy current density has decreased to  $1/e$  or 36.8% of the surface density. Also known as skin depth.

**Detect** - Discover or identify the presence of existence of something

**Detector** - A device that determines the presence of or measures the amount of energy, such as radiation.

**Differential Probe** - A probe having two sensing coils located side-by-side allowing it to convert a floating signals to a low voltage ground referenced signal to be displayed on a ground referenced oscilloscope.

**Direct Current (DC)** - Electrical current that flows in only one direction in a circuit.

**Discontinuity** - A break in the continuity of a medium or material.

**Domain** - A substructure in a ferromagnetic material within which all the elementary magnets (electron spins) are held aligned in one direction by interatomic forces; if isolated, a domain would be magnetically saturated.

**Eddy Currents** - Localized electric current induced in a conductor by a varying magnetic field.

**Eddy Current Inspection** - An electromagnetic technique used on conductive materials for crack detection or the rapid sorting of small components for either flaws, size variations, or material variation, as well as other applications.

**Eddy Current Method** - An electromagnetic NDT Method based on the process of inducing electrical currents into a conductive material and observing the interaction between the currents and the material.

**Eddy Current Scope** - A scope that uses little electrical currents call "eddy currents" to find defects in different materials.

**Eddy Current Testing (EC)** - An electromagnetic technique used on conductive materials for crack detection or the rapid sorting of small components for either flaws, size variations, or material variation, as well as other applications.

**EDGE Effect** - Signal obtained when a surface probe approaches the sample's edge.

**Effective Depth of Penetration** -Depth at which eddy current density drops off to 5% of the surface density.

**Electrical Contact** - Contact of two conductors allowing current to pass.

**Electrical Current** - The movement of electrons between atoms.

**Electrical Impedance** - The total opposition that a circuit presents to an alternating current.

**Electrical Noise** - Extraneous signals caused by externally radiated signals or electrical interferences within an ultrasonic instrument. A component of background noise.

**Electromagnetic Induction** - A process by which electrical current is induced in an electrical conductor by a changing magnetic field that acts upon the conductor.

**END Effect** - Signal obtained when an internal or encircling probe approaches the end of a tube or rod (Similar to edge effect).

**Error Analysis** - The process used to evaluate the total error throughout an experiment. This can be due to bias error, precision error as well as others.

**Evaluation** - The process of deciding the severity of a condition after an indication has been interpreted. Evaluation determines if the test object should be rejected, repaired or accepted. See indication and interpretation.

**External Discontinuities** - Surface irregularities which cause density variations on a radiograph. These are observable with the naked eye

**False Indication** - A test indication that could be interpreted as originating from a discontinuity but which actually originates where no discontinuity exists.

**Far Field** - The zone beyond the near field in front of the transducer in which signal amplitude decreases monotonically in proportion to distance from the transducer. Also called the Fraunhofer zone.

**Ferromagnetic** - It is a measure of coupling between the coil and test object.  
- Fraction of the test coil area filled by the test specimen.

**Ferromagnetic Materials** - Materials that can be magnetized.

**Ferrous** - Describing a metal that is more than 50% iron, such as steel, stainless steel, cast iron, ductile (nodular) cast iron, etc.

**Field Intensity** - A term used to describe the strength of the electromagnetic field.

**Filled Crack** - A crack-like discontinuity, open to the surface, but filled with some foreign material-oxide, grease, etc.- which tends to prevent penetrants from entering.

**Filter** -A device for suppressing electrical waves of frequency not required.

**Fine Crack** - A discontinuity in a solid material with a very fine opening to the surface, but possessing length and depth greater than the width of this opening; usually depth is many times the width.

**Flat Bottom Hole** - A type of reflector commonly used in reference standards. The end (bottom) surface of the hole is the reflector.

**Flaw** - A defect, blemish, imperfection.

**Flaw Reconstruction** - The process used to determine what a flaw looks like through non-destructive testing.

**Flux Density** - The number of flux lines per unit of area, measured at right angles to the direction of the flux. It is the measure of magnetic field strength.

**Flux Leakage** - Flux, or lines of force, leaking from pole to pole outside a magnet.

**Foucault Currents Method** - In France the eddy current method is known as the "Foucault Currents" method.

**Frequency** - The number of waves that pass a given point in a specified unit of time.

**Frequency, Fundamental** - In resonance testing, the frequency at which the wavelength is twice the thickness of the test material.

**Frequency, Pulse Repetition** - The number of pulses per second.

**Frequency Response** - The range of frequencies over which a device operates as expected.

**Function Generators** - A device that generates a function wave such as a sine wave or square wave.

**Gain Control** - the sensitivity control.

**Gate** - An electronic device for monitoring signals in a selected segment of the trace on an A-scan display.

- The interval along the baseline that is monitored.

**Grinding Cracks** - Shallow cracks formed in the surface of relatively hard materials because of excessive grinding heat or the high sensitivity of the material.

**Gross Porosity** - In weld metal or in casting, pores, gas holes or globular voids that are larger and in greater number than obtained in good practice.

**Harmonic** - A vibration frequency that is an integral multiple of the fundamental frequency.

**IACS(International Annealed Copper Standard)** - Conductivity as a percentage of pure copper.

**Impedance** - The effective resistance to an alternating electric current arising from the combined effects of ohm resistance and reactance

**Impedance Method** - Eddy current method, which monitors the change in probe impedance; both phase and amplitude.

**Impedance Plane** - The plane formed by the resistance component and the reactance component.

**Inclusion** - Non-metallic particles, usually compounds in a metal matrix. Usually considered undesirable, though in some cases, such as in free machining metals, inclusions may be deliberately introduced to improve machinability.

**Indication** - In non-destructive testing, the response from or the evidence of a discontinuity in material condition or structure.

**Induced Current** - Passing an alternating current through a conductor will set up a fluctuating magnetic field. If a second conductor in the form of a closed loop is placed in this field, the action of the fluctuating field moving across the conductor will set up a second alternating current of the same frequency. This is an induced current.

**Inductance** - Ratio of the total magnetic flux-linkage in a coil to the current flowing through the coil.

**Inductive Reactance** - The opposition to a change in alternating current flow.

**Inject** - Introduce, for example an electrical current into an electrical circuit

**Injection** - An act of injecting or being injected

**Interface** - The boundary between two contacting parts or regions or parts.

**Internal Probe (coil)** - A probe for testing tube (or holes) from the inside. The coil(s) is circumferentially wound on a bobbin.

**Interpretation** - The determination of the source and relevancy of an ultrasonic indication.

**Lift-Off** - The vertical take-off (lift – raise or the raised to a higher position or level)

**Lissajous figure** - A looped or curved figure traced out by a point undergoing two independent single harmonic motion at right angles with frequencies in a simple ratio.

**Magnetic Materials** - Materials are affected by magnetism in two general ways. Some of them are attracted by a magnet, while others exert a repellent force. The first is called "paramagnetic" and the later "diamagnetic." In Magnetic particle inspection we are not ordinarily concerned with either of the two classes, but with what may be termed a subdivision of the first class called "ferromagnetic materials."

**Metal** - An opaque, lustrous elemental chemical substance that is a good conductor of heat and electricity and, when polished, a good reflector of light. Most elemental metals are malleable and ductile and are, in general, heavier than the other elemental substances.

**Microfissure** - A crack of microscopic proportions.

**Multi-Frequency Techniques** - These kind of techniques simply involve collecting data at several different frequencies and then comparing the data or mixing the data in some way.

**Mutual Inductance** - When one circuit induces current flow in a second nearby circuit.

**NDE** - Acronym for **Non-destructive Evaluation**

**NDT**- Acronym for **Non-destructive Testing**.

**NDT Methods** - A process used to test an object for flaws and other defects that does not harm the object.

**Near Field** - The distance immediately in front of the transducer in which the ultrasonic beam exhibits complex and changing wavefronts. Also called the Fresnel Field or Fresnel Zone.

**Noise** - Any undesired signal that obscures the signal of interest.  
- It might be electrical noise or a signal from specimen dimensional or property variations.

**Non-destructive Evaluation (NDE)** - The use of non-invasive techniques to determine the integrity of a material, component or structure, or to quantitatively measure some characteristic of an object. (Making quantitative measurements is what distinguishes NDE from NDT.)

**Non-destructive Testing (NDT)** - Testing to detect defects in materials using techniques that do not damage or destroy the items being tested.

**Non-relevant Indication** - An indication that has no relation to a significant discontinuity.

**Oscilloscope** - A device that displays how a voltage or current signal varies over time.

**Permeability** - The ease with which a magnetic flux can be established in a given magnetic circuit.

**Permeability (Magnetic)** - Ratio between flux density, B, and magnetizing force, H. Permeability describes the intrinsic willingness of a material to conduct magnetic flux lines.

**Perturbation** - Any effect that causes a small change in a physical system and/or changes the value of some given function.

**Phase** – Relationship in time between the cycles of an oscillating or repeating system and a fixed reference point or a different system.

**Phase Angle** – A phase difference expressed as an angle

**Phase space** – A multidimensional space in which the axes correspond to the coordinates required to specify any state of a system

**Probe** - Eddy current transducer.

**Pulsed Eddy Current** - A test used for detection and quantification of corrosion and cracking

**Pulser-Receiver**- Used with a transducer and oscilloscope for flaw detection and thickness gauging.

**Radial** - In the direction of a radius between the center and the surface of a circle, cylinder, or sphere.

**Reactance** - The non-resistive component of impedance in an AC circuit arising from inductance and/or capacitance

**Reference Blocks** - A block or series of blocks of material containing artificial or natural discontinuities or one or more reflecting areas at one or more distances from the test surface, which are used for reference in defining the size and distance of defective areas in materials.

**Reference Coil** - Coil which enables bridge balancing in absolute probes. Its impedance is close to test coil impedance but does not couple to test material.

**Reference Standards** - A reference object containing known reflectors representing accept or reject criteria.

- A sample test object.

**Resistance (R)** - The opposition to the flow of electrical current. Measured in ohms

**Resistivity** - Reciprocal of conductivity.

**Resistors** - Components that are used to control that amount of current flowing in a circuit by adding a specific amount of resistance.

**Resolution** - The ability to clearly distinguish signals obtained from two reflective surfaces with a minimum difference in depth. Near surface resolution is the ability to clearly distinguish a signal from a reflector at a minimum distance under the near surface without interference from the initial pulse signal. Far surface resolution is the ability to clearly distinguish signals from the back surface when the sound beam is normal to that back surface.

**Saturation (Magnetic)** - A condition where incremental magnetic permeability of a ferromagnetic material becomes 1.0.

**Saturation Level** - The limit of indication height that is obtained as the area of the discontinuity is increased.

**Scanning** - Movement of the transducer over the surface of the test object in a controlled manner so as to achieve complete coverage. May be either contact or immersion method. Eddy current data can be collected using automated scanning systems to improve the quality of the measurements and to construct images of scanned areas.

**Send-Receive** - The variations in the test object which affect current flow within the test object can be detected by observing their effect upon the voltage developed across a secondary receive coil.

**Sensitivity** - A measure of the ability to detect small signals. Limited by the signal-to-noise ratio.

**Signal-to-Noise Ratio** - Ratio between defect signal amplitude and that from non-relevant indications. Minimum acceptable ratio is 3:1.

**Skin Depth** - See depth of penetration.

**Skin Effect** - A phenomenon where induced eddy currents are restricted to the surface of a test sample. Increasing test frequency reduces penetration.

**Solenoid** - An electrically charged coil of insulated wire which produces a magnetic field within the coil.

**Spectrum** - The amplitude distribution of frequencies in a signal.

**Spectrum Response** - The amplification (gain) of a receiver over a range of frequencies.

**Standard** - A reference object used as a basis for comparison or calibration.

- A concept established by authority, custom or agreement to serve as a model or rule in the measurement of quantity or the establishment of a practice or procedure.

**Subsurface Discontinuity** - Any discontinuity which does not open onto the surface of the part in which it exists. Not detectable by liquid penetrant inspection.

**Surface-Breaking Cracks** - Cracks formed on the surface of an object.

**Surface Probe** - A probe for testing surfaces, which has a finite coverage. The coil is usually pancake in shape.

**Test Coil** - Coil coupled to test material. It senses geometric, electric and magnetic changes in test material.

**Test Frequency** - The frequency  $f$  vibration of the ultrasonic transducer employed for ultrasonic testing.

**Test Surface** - That surface of the test object at which the ultrasonic energy enters or leaves.

**Threshold** - In reference to current or magnetic fields, the minimum strength necessary to create a looked-for effect is called the threshold value. For example, the minimum current necessary to produce a readable indication of a given defect is the threshold value of current for the purpose.

**Transducer** - A device that converts variation in a physical quantity into an electrical signal

**Transducer Element** - The component in a transducer that actually converts the electrical energy into acoustical energy and vice versa. The transducer element is often made of a piezoelectric material or a magnetostrictive material.

**Wavelength** - The distance needed in the propagation direction for a wave to go through a complete cycle.

## REFERENCES

- [1] GRIMBERG, R. UDPA, L., SAVIN, A., STEIGMANN, R. and UDPA, S., Inner Eddy-current Transducer with Rotating Magnetic Field. Theoretical Model – Forward Problem, Research in Nondestructive Evaluation, Springer-Verlag New York, LLC, vol. 16, issue 2, ISSN: 0934-9847 (2005).
- [2] GRIMBERG, R. UDPA, L., SAVIN, A., STEIGMANN, R. and UDPA, S., Inner Eddy-current Transducer with Rotating Magnetic Field; Experimental Results: Application to Nondestructive Examination of Pressure Tubes in PHWR Nuclear Power Plants, Research in Nondestructive Evaluation, Springer-Verlag New York, LLC, vol.16, issue 2 pp. 65-77, ISSN: 0934-9847 (2005).
- [3] GRIMBERG, R., UDPA, L., UDPA, S. and SAVIN, A., A Novel Rotating Magnetic Field Eddy-current Transducer for the Examination of Fuel Channels in PHWR Nuclear Power Plants, Review of Quantitative Nondestructive Evaluation vol. 24, ed. by D.O. Thompson and D.E. Chimenti © 2005, ISBN 0-7354-0245-0.
- [4] GRIMBERG, R., SAVIN, A. and STEIGMANN, R., Eddy-current Inner Transducer with Rotating Magnetic Field; Application to PHWR's Pressure Tubes, International Journal of Materials and Product Technology, ISSN: 0268-1900 (2005).
- [5] PRÉMEL, D., SAVIN, A. and GRIMBERG, R., Calculation of the Response of the Eddy-current Inner Transducer in the Presence of Copper and Magnetite Deposits and of Antivibration Railing, Studies in Applied Electromagnetics and Mechanics 21, Electromagnetic Nondestructive Evaluation (V), J. Pavo et al. (Eds.) IOS Press, pp. 22-29 ISBN: 1-58603-155-4 (2001).
- [6] PRÉMEL, D., SAVIN, A. and GRIMBERG, R. and MADAOU, N., Modelling the Operations of a New Type of Eddy-current Transducer for Non-destructive Evaluation of Tubes of Steam Generators, Studies in Applied Electromagnetics and Mechanics 17, Electromagnetic Nondestructive Evaluation (IV), S.S. Udpa et al. (Eds) IOS Press, pp. 42-49 ISBN: 1-58603-023-X (2000).
- [7] GRIMBERG, R., PRÉMEL, D., RADU, E. and SAVIN, A., Modelling the Operation of an Inside Eddy-current Transducer with a Rotating Magnetic Field, Studies in Applied Electromagnetics and Mechanics 18, Non-Linear Electromagnetic System, P. Di Barba and A. Savini (Eds) IOS Press, 293-296 ISBN: 1-58603-024-8 (2000).
- [8] GRIMBERG, R., SAVIN, A., CHIFAN, S. and RADU, E., The Inverse Problem for the Eddy-current Control with a Rotating Magnetic Field, Studies in Applied Electromagnetics and Mechanics 18, Non-Linear Electromagnetic System, P. Di Barba and A. Savini (Eds) IOS Press, 451-454 ISBN: 1-58603-024-8 (2000).
- [9] GRIMBERG, R., SAVIN, A. and STEIGMANN, R., Forward Problem for Eddy-current Inner Transducer with Rotating Magnetic Field; Application to Pressure Tubes from CANDU Nuclear Power Plant, 3rd International Conference on NDT of the Hellenic Society for NDT (HSNT), 15-17 October 2003, Chania, Crete-Greece, pp. 292-296 (2003).
- [10] CAN/CSA-N285.4-94, "Periodic Inspection of CANDU Nuclear Power Plant Components".
- [11] GHENT, H.W., A Novel Eddy-current Surface Probe", AECL Report AECL-7518 (1981).
- [12] HORN, D. and MAYO, W.R., NDE Reliability Gains from Combining Eddy-current and Ultrasonic Testing" NDT&E International vol. 33 pp. 351-362 (2000).

- [13] GRIMBERG, R., PRÉMEL, D., SAVIN, A. and STEIGMANN, R., Eddy-current Evaluation of Pressure Tubes from PHWR Power Plants, The 8th International Workshop on Electromagnetic Nondestructive Evaluation, June 12-14, 2002, Saarbrücken, Germany (2002).
- [14] GRIMBERG, R., SAVIN, A. and STEIGMANN, R., Forward Problem for Inner Eddy-current Transducer with Rotating Magnetic Field, The 10<sup>th</sup> International IGTE Symposium on Numerical Field Calculation in Electrical Engineering, 2002, Austria, IDN a711, ISBN 3-901351-65-5 (2002).
- [15] GRIMBERG, R., PRÉMEL, D., SAVIN, A. and CHIFAN, S., Eddy-current Inner Control of Amagnetic Pipes Using the Rotating Magnetic Field Method, Proceedings of the 15<sup>th</sup> World Conference of Non-Destructive Testing, Roma, Italy, 2000, IDN 521. The e-Journal of Nondestructive Testing & Ultrasonics vol. 5 No. 10 - October 2000 - ISSN: 1435-4934.
- [16] SAVIN, A., PRÉMEL, D., GRIMBERG, R. and LE BIHAN, Y., Evaluation of Delamination in Carbon Fibre Composites Using the Eddy-current Method, Proceedings of the 15<sup>th</sup> World Conference of Non-Destructive Testing, Roma, Italy, 2000, IDN 499. The e-Journal of Nondestructive Testing & Ultrasonics vol. 5 No. 10 - October 2000 - ISSN: 1435-4934 (2000).
- [17] SOARE, M. and IORDACHE, C., Performance Characterization of Nondestructive Methods for Flaw Detection and Sizing in CANDU Pressure Tubes. Part I: Ultrasonic Spectroscopy Investigations Using Longitudinal Waves for Interrogation, NNDT Report No. RCD-ICC-AIEA-27.1/2001 Rev. 1 (2001).
- [18] SOARE, M. and IORDACHE, C., Performance Characterization of Nondestructive Methods for Flaw Detection and Sizing in CANDU Pressure Tubes. Developed Methodology for Flaw Sizing, NNDT Report No. RCD-ICC-AIEA-27.11/2004 Rev. 0 (2004).

## CONTRIBUTORS TO DRAFTING AND REVIEW

|               |  |
|---------------|--|
| Belinco, C.G. | Comisión Nacional de Energía Atómica (CNEA-CAC), Argentina   |
| Chaplin, K.   | AECL Chalk River Laboratories, Canada  |
| Cheong, Y.-M. | Korea Atomic Energy Research Institute (KAERI), Republic of Korea  |
| Cleveland, J. | International Atomic Energy Agency   |
| Garcia, A.    | Comisión Nacional de Energía Atómica (CNEA-CAC), Argentina   |
| Grimberg, R.  | National Institute of Research & Development for Technical Physics, Iasi, Romania  |
| Jang, K.S.    | Korea Electric Power Research Institute (KEPRI), Republic of Korea   |
| Joulin, T.    | AECL Chalk River Laboratories, Canada  |
| Kim, Y.-S.    | Korea Electric Power Research Institute (KEPRI), Republic of Korea   |
| Kulkarni, P.  | Bhabha Atomic Research Centre, India   |
| Lee, H.-J.    | Korea Electric Power Research Institute (KEPRI), Republic of Korea   |
| Lyon, R.      | International Atomic Energy Agency   |
| Mayo, W.      | AECL Chalk River Laboratories, Canada  |
| Nanekar, P.   | Bhabha Atomic Research Centre, India   |
| Shah, B.K.    | Bhabha Atomic Research Centre, India   |
| Soare, M.     | S.C. Nuclear NDT Research & Services S.R.L. (NNDT), Romania  |
| Zhu, R.       | China National Nuclear Corporation, Research Institute of Nuclear Power Operation, Nuclear In-service Inspection Center, China |